参赛队员姓名：**Songtao Li**

中学：**Princeton International School of Mathematics and Science**

省份：**New Jersey**

国家/地区：**U.S.**

指导教师姓名：**Qiang Chen**

论文题目：**Green Synthesis of Titanium Dioxide/Polymer Nanocomposites with Enhanced Catalytic Activity**

Green Synthesis of Titanium Dioxide/Polymer Nanocomposites with Enhanced Catalytic Activity

Songtao Li[1]

[1] Princeton International School of Mathematics and Science, Princeton, NJ 08540

Abstract

Polymer nanocomposites, which incorporate advantages of both nanoparticles and polymers, have received increasing attention in both academia and industry. While inorganic nanoparticles dispersed in polymer matrices can enhance bulk properties, modifying the surface of inorganic nanoparticles with polymers can change its surface structure for various functional applications such as photocatalysis. In addition, the composites provide an effective approach to overcome the bottleneck problems of nanoparticles in practice such as separation and reuse. In this research, two TiO_2/polymer nanocomposites are prepared with the focus on simplifying the synthesis and avoiding the use of toxic chemicals. Two different approaches, grafting with polymer-based structures and immobilization in polymer matrix, are taken to achieve enhanced photocatalytic activities under visible light and enhanced recycling properties. Our findings provide insights into an economic, green, and facile route of preparing TiO_2/polymer nanocomposite with enhanced photocatalytic activity for practical applications. Key findings of this research are:

1. A facile and green method to synthesize Degraded-PVA coated TiO_2 (TiO_2@D-PVA) nanoparticles containing conjugated structures was prepared via physical mixing, centrifugation, and calcination. The content of D-PVA in TiO_2@D-PVA could be controlled by the concentration of the PVA solution. Under visible light irradiation, the TiO_2@D-PVA containing approximately 5 wt% D-PVA demonstrated an optimal photocatalytic activity which is 5.5 times higher than that of commercial P25 TiO_2 nanoparticles. The Ti-O-C bonds and the conjugated structures in D-PVA could facilitate the electron transfer between D-PVA and TiO_2, thus contributing to the enhanced visible light photocatalytic activity.
2. A polymer dots-grafted TiO_2/PVA porous composite film (p-PVA/PDs-TiO_2) was synthesized through immobilizing polymer dots grafted TiO_2 (PDs-TiO_2) nanoparticles synthesized via a two-step hydrothermal reaction onto a PVA film made porous via treatment of $CaCO_3$ particles introduced during solution casting with weak acid. The photocatalytic rate of p-PVA/PDs-TiO_2 under sunlight is approximately 2.74 times higher than the nonporous sample. The composite film demonstrated excellent stability after 3 cycles of 4.5 h each of AM 1.5 G simulated sunlight, with the rate constant decreasing by only approximately 5%.

Keywords: Titanium Dioxide, Photocatalytic Activity, Polyvinyl Alcohol (PVA), Nanocomposite

Table of Contents:

1. Introduction

1.1. Overview of TiO_2 Nanoparticles

1.1.1. Structure and property of TiO_2 nanoparticles

TiO_2, a typical transition metal oxide nanoparticle, exhibits three commonly known polymorphs in nature: brookite, rutile, and anatase [1]. Brookite TiO_2 belongs to the orthorhombic crystal system with a unit cell composed of 8 formula units of TiO_2 formed by edge-sharing TiO_6 octahedra. Comparatively little is known about the properties and photoactivities of the brookite phase since it is the rarest phase to be synthesized in the standard environment among TiO_2 polymorphs [2]. Rutile TiO_2 has a tetragonal structure and contains 6 atoms per unit cell with a slightly distorted TiO_6 octahedron. Generally speaking, the photocatalytic activity of rutile phase is relatively poor, but it is also dependent on the conditions of preparation [3]. Anatase TiO_2 also has a tetragonal structure but with a less distorted TiO_6 octahedron compared with rutile phase. The anatase phase is more stable than the rutile at 0 K, but the energy difference between these two phases is small (2 to 10 kJ/mol) [4]. Kinetically, anatase is stable at room temperature, but at a macroscopic scale, its transformation to rutile phase reaches a measurable speed for bulk TiO_2 at temperatures higher than 600 ˚C [5]. Due to surface energy effects, anatase is most thermodynamically stable at sizes less than 11 nm while brookite is most stable between 11 and 35 nm and rutile is most stable at sizes greater than 35 nm [6,7]. The higher photoreactivity of anatase may be attributed to a relatively lower Fermi level, a lower capacity to adsorb oxygen, and a higher degree of hydroxylation [8]. In addition, for an anatase crystal the reactivity of (001) facets is greater than that of (101) facets [9].

1.1.2. Synthesis of TiO_2 nanoparticles

The synthesis of TiO_2 nanoparticles can be roughly divided into liquid-phase synthesis and gas-phase synthesis.

Liquid-phase synthesis is one of the most convenient and utilized methods of synthesis. These methods have the advantage of controlling over the stoichiometry, producing homogeneous materials, allowing formation of complex shapes, and preparation of composite materials [5]. Typical examples are precipitation methods, solvothermal methods, and sol-gel methods. Precipitation method involves the addition of a basic solution to a precursor, usually $TiCl_3$, $TiCl_4$ or $Ti(SO_4)_2$, to precipitate the amorphous $Ti(OH)_4$ [10–12]. After separation and calcination to crystallize the TiO_2, the anatase phase is usually produced despite use of sulfate or chloride [10–12]. Solvothermal methods feature chemical reactions in aqueous or organic media under self-produced pressures at low temperatures (usually under 250 ˚C) using precursors such as $TiOSO_4$ or $TiCl_4$ [5,13–15]. The grain size, particle morphology, crystalline phase, and surface chemistry of the TiO_2 can be controlled through regulating the solution composition, reaction temperature, pressure, and etc.

The sol-gel method involves the formation of a TiO_2 sol or gel or precipitation by hydrolysis and condensation (with polymer formation) of titanium alkoxides from titanium sources such as $Ti(O\text{-}Et)_4$, $Ti(O\text{-}i\text{Pr})_4$, and $Ti(O\text{-}n\text{Bu})_4$ [16–18].

Gas phase methods are commonly used to deposit TiO_2 thin films as well as nanoparticle powder. Typical gas phase methods include chemical vapor deposition, physical vapor deposition, and spray pyrolysis deposition. Chemical vapor deposition features chemical reactions or decomposition of a precursor, ranging from metals to composite oxide, in the gas phase to yield the desired product [19]. Physical vapor deposition is commonly used to create films are formed from the deposition gas-phase TiO_2 [20]. Spray pyrolysis deposition is an alternate aerosol deposition technique related to CVD but is different mainly in that an aerosol is used instead of vapor as the precursor [21].

1.1.3. Surface modifications of TiO_2 nanoparticles

Through surface modification of TiO_2 nanoparticles, the surface activity, photostability, and compatibility with solvents can be improved while allowing for the addition of novel properties to the surface of the nanoparticles. Zhao *et al.* modified TiO_2 nanoparticles with silane coupling reagents and found that the particle dispersion stability was positively affected by an increase in particle zeta potential [22]. In addition, the silane coupling reagent was chemically bonded onto the surface of the TiO_2 nanoparticles, and the photocatalytic activity of the composite was dependent significantly on the organosilane ratio. Lu *et al.* developed a method to modify TiO_2 nanoparticles through surface-grafting L-lactic acid oligomer in the presence of stannous octanoate [23]. The grafted TiO_2 was evenly dispersed in the polymer matrix, and the tensile strength and ductility of the grafted polymer were also significantly improved compared to the non-grafted composite. Lou *et al.* used surface carboxylated TiO_2 nanoparticles to improve the dispersity of nano-TiO_2 particles in PVA and to enhance the interaction between nanofiller and matrix, and found that through increasing surface carboxylation the tensile strength and storage modulus was significantly increased due to the high dispersion and the crosslinking present between PVA and carboxylated TiO_2 nanoparticles [24].

1.2. Photocatalytic properties of TiO_2 nanoparticles

1.2.1. Mechanism of photocatalysis

TiO_2 is an n-type semiconductor with relatively large band gaps of 3.2, 3.02, and 2.96 eV respectively for the anatase, rutile and brookite phases [1]. The valence band of TiO_2 is composed of the 2p orbitals of oxygen hybridized with the 3d orbitals of titanium, while the conduction band is only the 3d orbitals of titanium [25]. When TiO_2 is exposed to near-UV light, electrons in the valence band are excited to the conduction band leaving behind holes (h^+) [5]. Hydroxyl radicals are formed on the surface of TiO_2 by the reaction of holes in the valence band with adsorbed H_2O, hydroxide, or surface titanol groups (-TiOH) [5]. The photogenerated electrons are reduced enough to produce superoxide (O_2^{2-}). This superoxide is an effective

oxygenation agent that attacks neutral substrates as well as surface-adsorbed radicals and/or radical ions [5]. In theory, the redox potential of the electron–hole pair permits H_2O_2 formation by either water oxidation or by reduction of the adsorbed oxygen with two conduction band electrons [5]. After the interfacial charge transfer reactions, the radical ions can participate in various pathways in the photomineralization process, including reacting chemically with themselves or surface-adsorbed compounds, recombining by back electron-transfer reactions, or diffusing from the semiconductor surface and participate in chemical reactions in the bulk solution [5].

1.2.2. Applications of TiO_2 nanoparticles in water treatment

Since 1976 when Carey *et al.* first reported the degradation of polychlorobiphenyls under the presence of TiO_2, photocatalysis with TiO2 nanoparticles has been shown useful for the degradation of wastewater pollutants [26]. Due to its low cost and high reactivity, TiO_2 has been widely applied for photomineralization of various organic pollutants into non-toxic small molecules such as CO_2 and H_2O.

Oil derivatives are one of the most dangerous pollutants due to their ability to migrate both in water and on land. Through coating hollow glass microbubbles with microcrystalline TiO_2 and surface modification to allow for oleophilic surfaces, a rate adequate for maintaining the surface of the water of a harbor, ship channel, coast, or lake free of an oily sheen, or for oxidative stripping of a film from minor spillage common in transfer of oil at terminals can be achieved [27].

Today, effluents of a large variety of industries usually contain important quantities of synthetic organic dyes which would cause considerable non-aesthetic pollution and serious health-risk when discharged [28]. Studies have reported that there are more than 100,000 commercially available dyes with an estimated annual production of over 7×10^5 tons of dye-stuff [29]. Epling studied the kinetics of photocatalytic degradation of 15 types of organic dyes under visible light and found that the rates of the pseudo first-order reaction differ significantly from families of dyes with different functionalities [30].

From sources such as industrial effluents and agricultural runoff, numerous types of pesticides are introduced into the water systems. A wide variety of pesticides is nowadays introduced into water systems from various sources such as industrial effluents, agricultural runoff, and chemical spills [5]. Because of their persistence in the aquatic environment and potential adverse health effects, the pesticide pollution of surface water and groundwater has been recognized as a major problem in many countries [31]. Various literature has reported the use of TiO_2 to degrade various types of pesticides, including s-trazines, organophosphates, phenylureas, and sulfonylureas [32–35].

1.2.3. Loading of TiO_2 nanoparticles

In order to prevent the loss during recycling and to improve the effective specific surface area, various researches have loaded TiO_2 nanoparticles onto various matrices for more efficient utilization. In addition, through dispersion within the matrix the

efficiency of utilizing the light source can be improved while also improving the physical adsorption of pollutants. Thus, an ideal matrix for loading TiO_2 nanoparticles should be transparent, can chemically bond with TiO_2 nanoparticles, have a large specific area for effective adsorption of pollutants, and is stable under the photocatalytic conditions in the presence of TiO_2 nanoparticles. In the past decades, researchers have utilized various methods, such as sol-gel method, chemical vapor deposition, and electrochemical deposition to load TiO_2 nanoparticles into various matrices [36–38]. The loading can be achieved through physical adsorption, electrostatic attraction, hydrogen bonding, and chemical bonding between the TiO_2 nanoparticles and the desired matrix, which may be inorganic (e.g. glass, ceramic, metal, and other adsorbents) or organic (e.g. carbon fiber, polymers) [37–43].

1.2.4. Visible light photocatalytic activity of TiO_2 nanoparticles

Due to its semiconductive properties, low cost, and biocompatibility, TiO_2 nanoparticles have become one of the most widely utilized photocatalysts for degradation of various pollutants. However, due to the relatively large band gap (3.0-3.2 eV), TiO_2 can only absorb ultraviolet light (UV) which covers only 4% of the solar spectrum [44]. Thus, various methods have been developed to enhance its photocatalytic activity under visible light.

Doping TiO_2 with various metal ions is one of the most commonly applied methods to engineer the visible light photocatalytic activity. Through replacing the atoms in the TiO_2 lattice, a bathochromic shift, i.e., a decrease of the band gap or introduction of intra-band gap states is introduced, which results in the increased absorption of more visible light and thus enhance the efficiency of the photocatalytic systems [1,5]. A huge variety of elements can be used as a dopant to improve the reactivity of TiO_2. Doping with transition metal ions provides additional energy levels within the band gap of the semiconductive TiO_2 and dopants such as Fe(III), Mo(V), Ru(III), Os(III), Re(V) and V(V) have been found to substantially enhanced the photochemical reactivity of TiO_2 [45]. Nobel metals can also be used to modify TiO_2 through suppressing electron-hole recombination as photoexcited electrons can be transferred from the conduction band of TiO_2 to metal particles deposited on the surface of TiO_2 while the holes remain in the valence band of TiO_2. Noble metals including Pt, Ag, Au, Pd, Ni, Rh, and Cu have been reported to be very effective at enhancing photocatalysis by TiO_2 [46–49]. Meanwhile, other studies have developed visible-light responsive TiO_2 through doping with various anions, as the mixing of the p states of the doped anion (N, S, F, or C) with the O 2p states shifts the valence band edge upwards and narrows the band gap energy of TiO_2 [50–52].

Dye sensitization is also extensively employed to enhance the efficiency of the excitation process and expand the wavelength range of excitation for TiO_2. The dye sensitizer attached to the surface of TiO_2 may inject either a hole or more commonly an electron to the TiO_2 nanoparticle upon photoexcitation, thus increasing the range of wavelength response of the photocatalyst [1,5]. Through forming a dye monolayer on the surface, the efficiency of charge injection into TiO_2 can be greatly enhanced [1,5]. Dyes and metal complexes that are used as sensitizers include erythrosin B, thionine,

substituted and unsubstituted bipyridine and phthalocyanine [53–56]. Due to its low fabrication cost, eco-friendly production and competitive efficiency, dye-sensitized TiO_2 has been widely applied in photovoltaic cells and photocatalyzed water-splitting [57–60]. Through coupling with another semiconductive nanoparticle, the photocatalytic activity of TiO_2 nanoparticles can be significantly improved through facilitating the charge separation, increasing the lifetime of charge carriers, and enhancing interfacial charge transfer to adsorbed substrates thus extending the energy range of photoexcitation [1,5]. Under photoexcitation, either one semiconductor or both can be illuminated. In the first case, the coupled semiconductor serves in a mechanism similar to as a sensitizer while in the second case both electrons and holes transfer between the semiconductors, with electrons accumulating at the lower lying conduction band of one semiconductor and the holes accumulating at the valence band of the other semiconductor [5]. Various semiconductor particles, such as CdS, Bi_2S_3, WO_3, SnO_2, MoO_3, and Fe_2O_3 have been used to enhance the photocatalytic activity of TiO_2 [61–64].

1.2.5. Polymer/TiO_2 Nanocomposites

Recently, polymers have been increasingly applied as a method of enhancing the photocatalytic activity of TiO_2 nanoparticles. Two different approaches are commonly used to modify TiO_2 with conjugated structures in which the photogenerated π–π^* transition allows for the transfer of excited electrons into the conduction band of TiO_2, then yielding reactive oxygenous radicals to degrade pollutants.

The first method directly grafts conjugated structures onto the TiO_2 nanoparticles. While conjugated polymers and dye sensitizers are both organic semiconductors, compare to dye sensitizers conjugated polymers is preferred in that it has a lower solubility in water, is more stable under photocatalytic degradation, and can facilitate the adsorption of pollutants. Zhang *et al.* grafted TiO_2 nanoparticles with a monolayer dispersed polyaniline via a facile chemisorption approach [65]. The observed increase in both the visible light and ultraviolet photocatalytic activity may be attributed to the migration efficiency of photogenerated carriers on the interface of polyaniline and TiO_2 [65]. Lin *et al.* prepared a nanometer TiO_2/poly-(fluorene-co-thiophene) photocatalyst and found that the degradation of phenol using the synthesized photocatalyst was much higher than it was using TiO_2/rhodamine B [66]. Liang *et al.* prepared a polythiophene-TiO_2 nanotube film by a two-step electrochemical process of anodization and electropolymerization, and the as-prepared films revealed significant activity for 2,3-dichlorophenols degradation under visible light irradiation and sunlight irradiation [67]. However, the application of such methods has been limited by the relatively high cost of conjugated polymers and complex process of polymerization.

Alternately, such conjugated structures on the surface of TiO_2 can be synthesized through controlled degradation of polymer-TiO_2 nanocomposites. Compared to the previous method of directly grafting conjugated polymers, this method is less expensive and is less tedious in operation. Min *et al.* fused a sol-gel method to obtain a TiO_2/Polyvinyl chloride composite and obtained a TiO_2/conjugated polymer

complex photocatalyst with some interaction between conjugated polymer and TiO_2. It was found that the conjugated polymer played an important role in enhancing photocatalytic degradation of methylene blue under visible light, and the temperature of calcination played an important role in determining the extent of conjugation and thus photocatalytic activity [68]. Wang *et al.* prepared a visible light active TiO_2/degraded polyvinyl alcohol photocatalyst by means of one-pot hydrothermal reaction between polyvinyl alcohol and $Ti(OH)_4$ [69]. The observed visible-light photocatalytic degradation of methyl orange in first-order kinetics was attributed to the interaction of D-PVA and TiO_2 [69].

1.3. Research Overview

In this research, the synthesis of TiO_2/polyvinyl alcohol nanocomposites is improved with the focus on green and facile synthesis. Through modifying TiO_2 with polymer the visible-light photocatalytic activity of TiO_2 is significantly improved, while its recycling stability is enhanced through loading in a polymer matrix. In addition, the synthesis of such polymer nanocomposites is designed to feature green and nontoxic chemicals and take significantly less time and effort compared to previous methods, which is crucial to the application of using sunlight to degrade pollutants in a real-life scenario.

In Section 2 of this paper, polyvinyl alcohol is selected to create a TiO_2@ conjugated degraded polymer core@shell nanoparticle. Through direct physical dispersion, centrifugation, and calcination, the degraded polyvinyl alcohol layer was chemically grafted evenly onto the TiO_2 nanoparticles. The thickness of the degraded polyvinyl alcohol shell is controlled and optimized through the concentration of the polyvinyl alcohol solution used, and the mechanism of the enhanced visible-light photocatalytic activity is discussed.

In Section 3 of this paper, the TiO_2 coupled with nanosized polymer dots are hydrothermally synthesized in-situ with polymer dot solution. The nanoparticles are then loaded onto a transparent polyvinyl alcohol thin film that is made porous on a microscale level through dissolving the calcium carbonate particles dispersed in the matrix. In this way, the final nanocomposite film is not only active under visible light and sunlight but also is stable under multiple cycles of repeated photocatalytic degradation of dye pollutants.

2. Facile green synthesis of Degraded-PVA coated TiO_2 nanoparticles with enhanced photocatalytic activity under visible light

2.1. Introduction

Since the success of hydrogen production through titanium dioxide (TiO_2) photocatalyzed water-splitting by Fujishima and Honda in 1972, TiO_2 has been widely used in the fields of air purification, sewage treatment, water splitting, reduction of CO_2, and dye sensitized solar cell because of its low cost, nontoxicity, and long-term stability [70–74]. However, due to the relatively large band gap (3.0-3.2 eV), TiO_2 can only absorb ultraviolet light (UV) which covers only 4% of the solar spectrum [44]. Therefore, over the past decades, considerable efforts have been directed toward the improvement of the photocatalytic efficiency of TiO_2 in visible light region, including doping with various metals and nonmetals, loading with noble metal particles, coupling with narrow bandgap semiconductors, grafting with conjugated structures, and etc. [70,72,75,76]. In the last decade, there is a growing interest in grafting conjugated structures onto the surface of TiO_2 nanoparticles since the conjugated structures can harvest visible light and inject excited electrons into the conduction band of TiO_2 [70,72,74]. Therefore, many conjugated structures, such as graphite-like carbon [77], fullerene [78], grapheme [79], commercial dye [80], carbon nanotubes [81], chlorophyll [82], fluorescein [83], and polypyrrole [84] have been utilized for improving the visible light photocatalytic activity of TiO_2.

Polyvinyl alcohol (PVA) is widely used in the fields of fiber, dispersant, glue and film because of its cheapness and nontoxicity. Under high temperature, PVA can form conjugated structures through elimination of adjacent side groups [70,72,74,85]. Therefore, there have been several attempts to graft conjugated structures onto the surface of TiO_2 by using PVA. Wang *et al.* [69] prepared $Ti(OH)_4$ precursor from titanyl sulfate and sodium hydroxide, and synthesized TiO_2/D-PVA microscale particles via hydrothermal treatment of $Ti(OH)_4$ and PVA solution. They found that PVA could dehydrate to produce conjugated unsaturated D-PVA and TiO_2/D-PVA exhibited high visible light photocatalytic activity. Lei *et al.* [72] developed a Conjugation-grafted-TiO_2 with high photocatalytic activity under visible light. PVA was first coated onto the commercial P25 TiO_2 nanoparticles via phase separation with ethanol, a nonsolvent of PVA. The products were separated, washed, and then calcinated to yield conjugated structures. Using the similar method based on phase separation and calcination, Filippo *et al.* [74] synthesized TiO_2/PVA hybrid nanoparticles which demonstrated an improved photocatalytic activity under visible light irradiation. Guo *et al.* [85] also prepared a conjugated-grafted-TiO_2 nanohybrid by grafting conjugated structures on the surface of nanotube titanic acid precursor-based TiO_2 through phase separation and thermal degradation of PVA. By calcinating TiO_2 sol and thermally treated PVA solution on glass substrates, Yang *et*

al. [86] prepared a PVA/TiO_2 composite film with visible-light photocatalytic activity. Li *et al* [70] synthesized Polymer dots (PDs) by hydrothermal treatment of PVA, and PDs-TiO_2 nanohybrids were prepared by hydrothermal treatment of PDs and $Ti(SO_4)_2$. They found that PDs-TiO_2 demonstrated excellent photocatalytic activity under visible light irradiation. These researchers found that the interfacial Ti-O-C bonds and the conjugated structures can act as the pathways to quickly transfer the excited electrons between conjugated structures and TiO_2, therefore contribute to the excellent photocatalytic activity [69,70,72,74,85].

However, the methods used for grafting PVA-based conjugated structures onto the surface of TiO_2 nanoparticles in previous studies usually involve several tedious treatment steps and large amounts of organic solvents [69,70,72,74,85,86]. Therefore, developing a facile, rapid, and green method to synthesis TiO_2/conjugated structures composite photocatalysts with visible light response remains highly desirable in terms of their large-scale applications.

In this research, a facile and green method to synthesize Degraded-PVA coated TiO_2 (TiO_2@D-PVA) nanoparticles containing conjugated structures was prepared. This method avoided using organic solvent and successfully coated D-PVA onto the surface of TiO_2 just via physical mixing, centrifugal and calcination. The morphology, structure, and photocatalytic properties of TiO_2@D-PVA were investigated in detail and a possible mechanism of the improved photocatalytic activity was proposed.

2.2. Experimental

2.2.1. Materials

Polyvinyl alcohol (PVA, average polymerization degree of 1750 ± 50) was purchased from Beijing Yili Fine Chemical Co., China. TiO_2 (P25, 20% rutile and 80% anatase) with a mean diameter of 21 nm was provided by Evonik Industries, Germany. Methyl orange (MO), used as the model pollutant, was manufactured by Zhejiang Yongjia Fine Chemical Plant, China. All chemicals were used without further purification.

2.2.2. Synthesis of TiO_2@D-PVA

3 g P25 was mixed with 150 mL 1 wt% PVA solution in a 250 mL beaker under continuously stirring for 0.5 h. Then, the suspension was centrifuged at 10, 000 rpm for 5 minutes. The deposit was calcinated at 220 °C for 2 h. After grinding, a brown product was got and named TiO_2@D-PVA-1. The excess PVA solution could be recovered and reused.

To investigate the effect of the D-PVA content on the photocatalytic activity of TiO_2@D-PVA, reactions with different content of PVA solution have been done by the same method. The products were labeled as TiO_2@D-PVA-*x*, where *x* is the concentration of PVA solution (*x*=0.5, 1, 2, 4). The weight loss of PVA was about 15.2% after calcinated at 220 °C for 2 h, indicating that about 37.1% hydroxyl groups in PVA were removed to form C=C bonds.

2.2.3. Characterization

The morphology of the TiO_2@D-PVA was characterized by a transmission electron microscope (TEM, HT7700, Hitachi) and a field emission scanning electron microscope (SEM, SU8020, Hitachi) equipped with an Energy diffusive X-Ray elemental analysis (EDX). Thermal gravimetric analysis (TGA) was carried out using Perkin-Elmer Pyris 1 under air atmosphere with air flow of 40 mL/min. About 3 mg sample was heated up to 700 ^{o}C at a heating rate of 20 ^{o}C/min. Fourier transform infrared (FT-IR) spectra were recorded on a Thermo Nicolet 6700 spectrophotometer equipped with an attenuated total reflectance device (Smart Orbit), the resolution of the spectra was 4 cm^{-1}, and scans were repeated 32 times. Photoluminescence (PL) measurements were performed at room temperature with a F-4500 fluorescence spectrometer (Hitachi). The UV-Vis Diffuse Reflectance spectra were recorded with a UV-Vis spectrophotometer (UV-2600, Shimadzu).

2.2.4. Photocatalytic Degradation

The photocatalytic degradation activity of the synthesized TiO_2@D-PVA was evaluated via the degradation rate of MO solution of 15 mg/L. 40 mL of the MO solution was mixed with the sample containing 20 mg TiO_2 in a 50 mL container. Prior to visible light irradiation, the sample was ultrasonically dispersed and was placed in dark under magnetic stirring for 1 h to achieve adsorption-desorption equilibrium. The light source was a 500 W halogen lamp equipped with an ultraviolet cut off filter (λ > 420 nm), the average visible light intensity measured with a radiometer was 130±10 mW/cm^2. The lamp was put in a cylindrical glass vessel with a recycling water glass jacket to make sure that the mixed solution was kept at room temperature. At regular time intervals, 5 mL suspension was filtered via a 0.22 μm syringe filter and the solution was examined by measuring the absorption at 465 nm using an UV-Vis spectrophotometer. MO degradation efficiency was calculated by the ratio of concentration (C_t/C_0, C_t, and C_0 can be calculated by the absorbance intensity).

2.3. Results and Discussion

2.3.1. Characterization of TiO_2@D-PVA nanoparticles

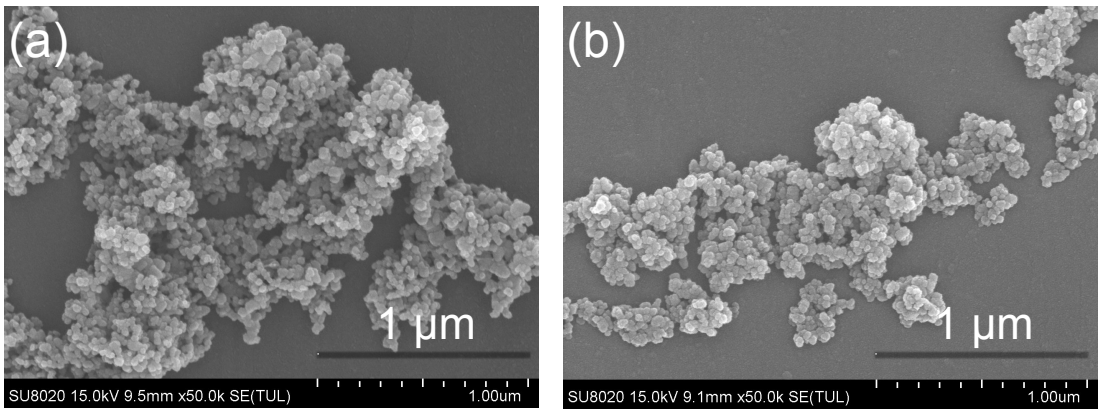

Fig. 1 SEM images of P25 (a) and TiO_2@D-PVA-1(b)

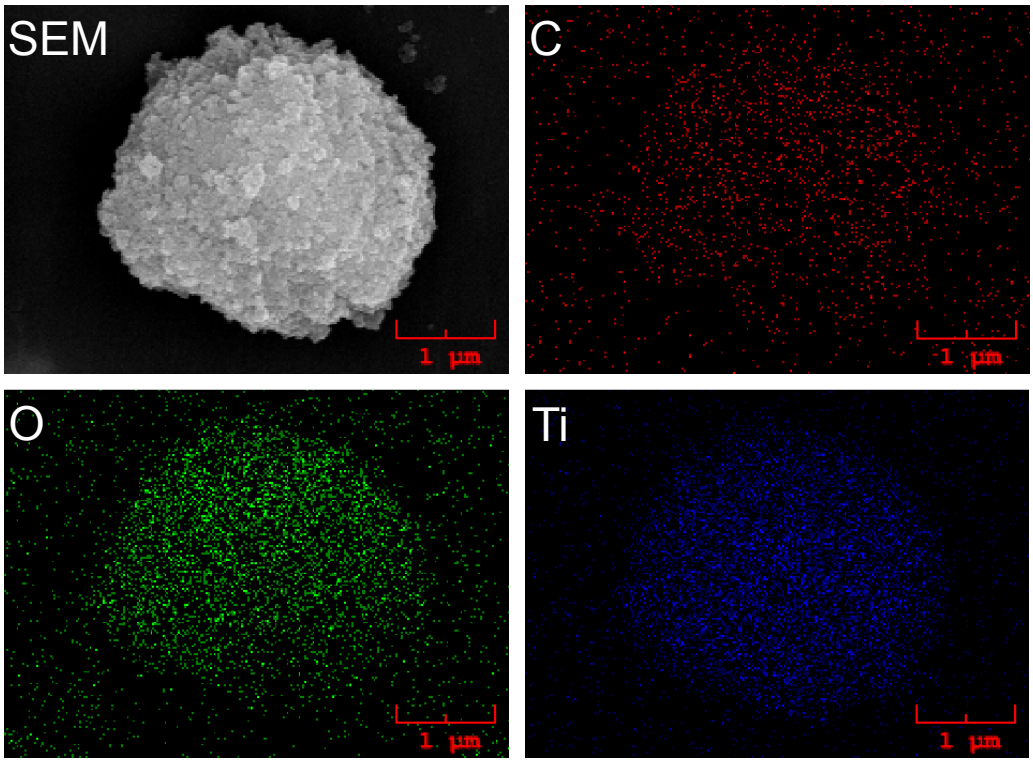

Fig. 2 EDX images of TiO_2@D-PVA-1

In order to investigate the morphology of TiO_2@D-PVA-1 nanoparticles, SEM was employed. As shown in Fig. 1(a), it can be seen that the P25 nanoparticles have a size of approximately 20 nm, which is in good agreement with previous literature [72,74]. Despite the TiO_2@D-PVA-1 in Fig. 1(b) has physical aggregation, it can be observed that the TiO_2@D-PVA-1 nanoparticles demonstrate a similar size around 20 nm, which implies that the D-PVA modification does not demonstrate a significant impact on the particle size of TiO_2 nanoparticles. EDX spectrum was taken to confirm the coating of D-PVA onto the surface of TiO_2 nanoparticles via the distribution of the C, O, and Ti elements [40]. As shown in the Fig. 2, a good correlation between the occurrence of C element with the occurrence of Ti and O elements can be observed. In addition, the distribution of C, O, and Ti elements are in good agreement with the distribution of the TiO_2@D-PVA-1 nanoparticles on the background. Thus, it can be concluded that the D-PVA is evenly coated onto the surface of P25 TiO_2 nanoparticles.

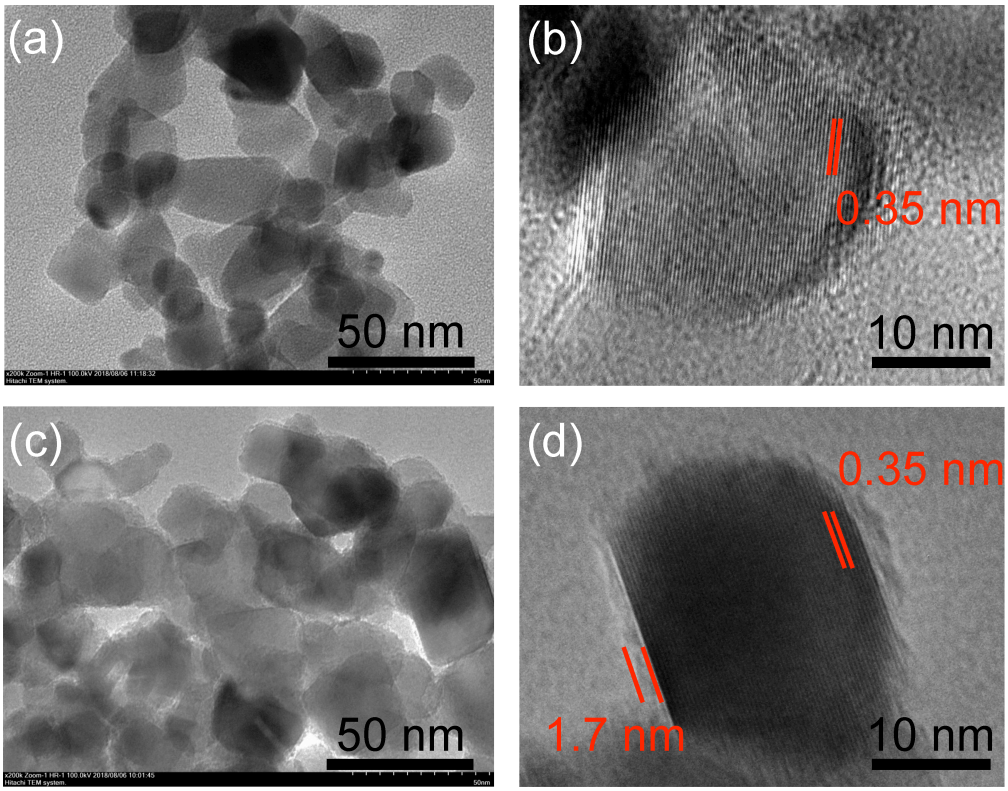

Fig. 3 TEM and HR-TEM images of P25 (a, b) and TiO_2@D-PVA-1 (c, d)

TEM was used to further investigate the morphological differences between TiO_2@D-PVA and P25. The surface of P25 is smooth and sharply defined with a size of about 20 nm in Fig. 3(a), a lattice spacing of 0.35 nm corresponding to the (101) crystal plane of anatase TiO_2 can be observed in the Fig. 3(b) [40,70]. However, for the TiO_2@D-PVA, a rugged D-PVA coating that is distributed evenly on the surface of TiO_2 can be observed in Fig. 3(c). The HR-TEM image in Fig. 3(d) shows that the thickness of the D-PVA coating is about 1.7 nm, which is in agreement with the optimal carbon layer thickness of 1-2 nm suggested by previous literature [77]. Furthermore, a similar 0.35 nm lattice spacing corresponding to the (101) crystal plane of anatase TiO_2 can also be observed in the TiO_2@D-PVA, this demonstrates that the D-PVA coating does not affect the crystal structure of the internal P25 TiO_2 nanoparticles [40,70].

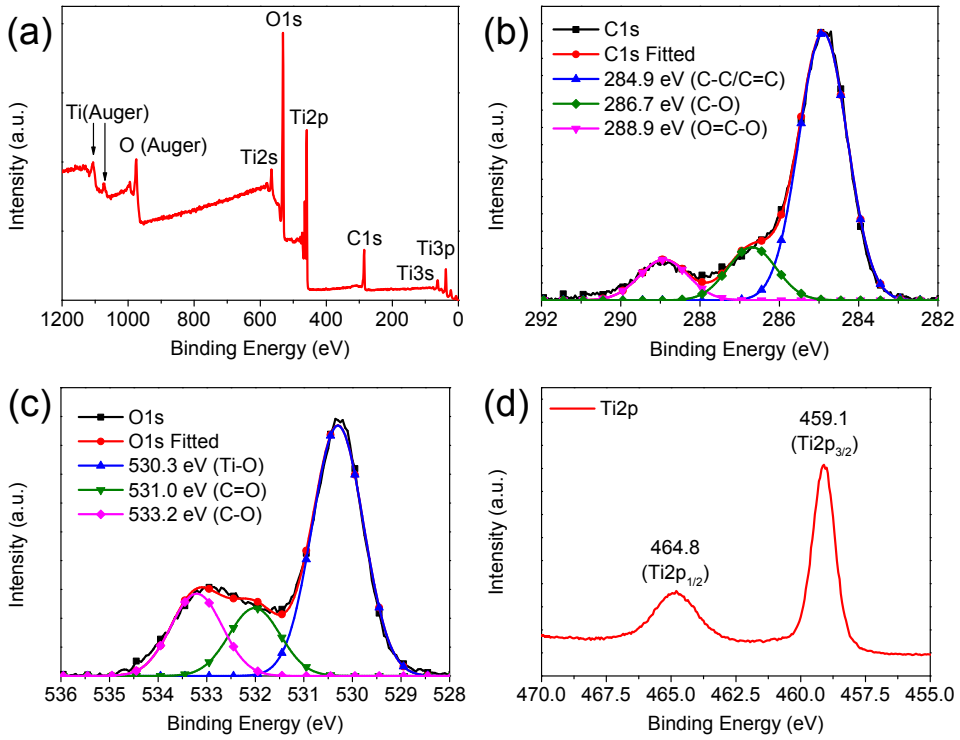

Fig. 4 (a) The full-scale XPS spectrum of TiO_2@D-PVA-1, High resolution XPS spectra of C1s(b), O1s(c), and Ti2p(d).

In order to further illustrate the interaction of D-PVA and P25, XPS was performed on the TiO_2@D-PVA. As shown in Fig. 4(a), the full-scale XPS spectrum shows the existence of Ti, O, and C in the TiO_2@D-PVA, which is in good agreement with the result of the EDX spectrum. The deconvoluted C1s XPS spectrum of the TiO_2@D-PVA is presented in Fig. 4(b). The peaks at 284.9 eV, 286.7 eV, and 288.9 eV are attributed to the carbon atoms in C-C/C=C, C-O, and O=C-O bonds respectively [70,72,86,87]. Therefore, it can be confirmed that conjugated D-PVA structures are present in the TiO_2@D-PVA, which is well consistent with the TEM results. The O1s XPS spectrum are shown in Fig. 4(c), the peaks at 530.3 eV, 531.0 eV, and 533.2 eV are attributed to the oxygen atoms in Ti-O, C=O, and C-O respectively, further confirming the D-PVA coating in TiO_2@D-PVA [70,72,86,87]. The peaks at 459.1 eV and 464.8 eV in Ti2p XPS spectrum in Fig. 4(d) are attributed to the typical peaks of $Ti2p_{3/2}$ and $Ti2p_{1/2}$, which indicates that the procedure of coating D-PVA does not affect the structure of the P25 TiO_2 nanoparticles [70,72,86,87].

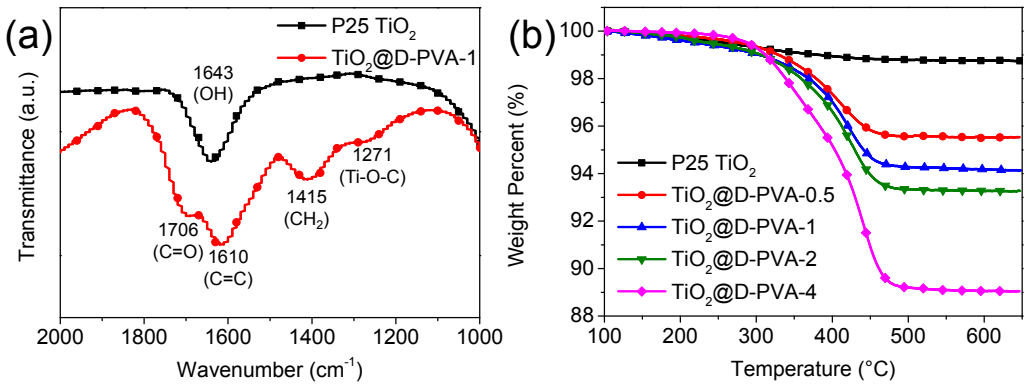

Fig. 5 (a) FT-IR spectra of P25 and TiO_2@D-PVA-1 (b) TGA of TiO_2@D-PVA samples

As shown in Fig. 5(a), FT-IR was employed to further confirm the structure of TiO_2@D-PVA-1. For P25, only one peak at 1643 cm^{-1} is observed and this peak is attributed to the bending vibration of the O-H bonds from the physically adsorbed water and surface hydroxyl groups [70]. In contrast, several new peaks at 1706 cm^{-1}, 1610 cm^{-1}, and 1415 cm^{-1} are observed on TiO_2@D-PVA-1. These peaks are attributed to the C=O stretching, conjugated C=C stretching, and CH_2 bending vibration in the D-PVA structures [70,72]. In particular, a relatively weak peak at 1271 cm^{-1} is observed and is attributed to the C-O-Ti bonds vibration, thus confirming a successful chemical bonding of D-PVA coating with the P25 TiO_2 nanoparticles respectively [70,72,74]. In addition, TGA was used to evaluate the actual content of D-PVA in TiO_2@D-PVA samples. As shown in Fig. 5(b), it can be observed that the samples prepared with different concentrations of PVA solution exhibit different contents of D-PVA. The loading content of D-PVA in TiO_2@D-PVA-0.5, TiO_2@D-PVA-1, TiO_2@D-PVA-2, and TiO_2@D-PVA-4 are 3.21 wt%, 4.61 wt%, 5.48 wt%, and 9.69 wt%, respectively. Thus, the D-PVA loading content in TiO_2@D-PVA can be controlled by the concentration of PVA solution.

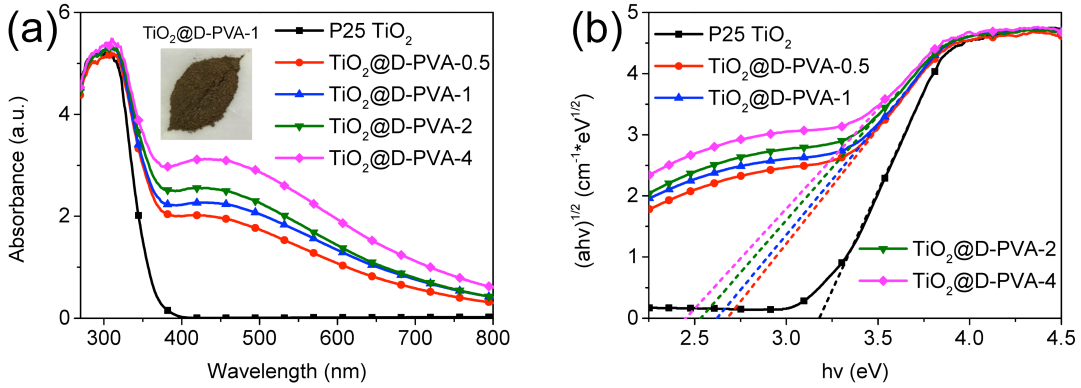

Fig. 6 (a) UV-Vis diffuse reflectance spectra of TiO_2@D-PVA samples (inset: photograph of TiO_2@D-PVA-1 powder). (b) Plots of transformed Kubelka-Munk function versus the energy of absorbed light.

Photoabsorption is one of the key factors affecting the photocatalytic

performance of photocatalysts. As in Fig. 6(a), pure P25 TiO_2 demonstrates a negligible absorption in the visible light region above 400 nm, while the prepared TiO_2@D-PVA samples show an obvious absorption of visible light. More specifically, the more D-PVA in TiO_2@D-PVA sample, the more visible light the sample absorbs. The photograph of TiO_2@D-PVA-1 powder demonstrates that the TiO_2@D-PVA has a brown color while the color of pure TiO_2 is white. In addition, as shown in Fig. 6(b), the bandgap energies of pure TiO_2 and TiO_2@D-PVA samples were calculated via the transformed Kubelka-Munk functions, and it is obvious that all of the TiO_2@D-PVA samples demonstrate a lower bandgap energy compared to the 3.18 eV bandgap of pure P25 TiO_2. Similarly, the bandgap energies of the TiO_2@D-PVA samples (2.68 eV, 2.62 eV, 2.53 eV, 2.45 eV) demonstrate a negative correlation with the D-PVA loading content. Such decrease of the bandgap may lead to the enhanced photocatalytic activity of TiO_2@D-PVA under visible light irradiation.

3.2. Photocatalytic activity

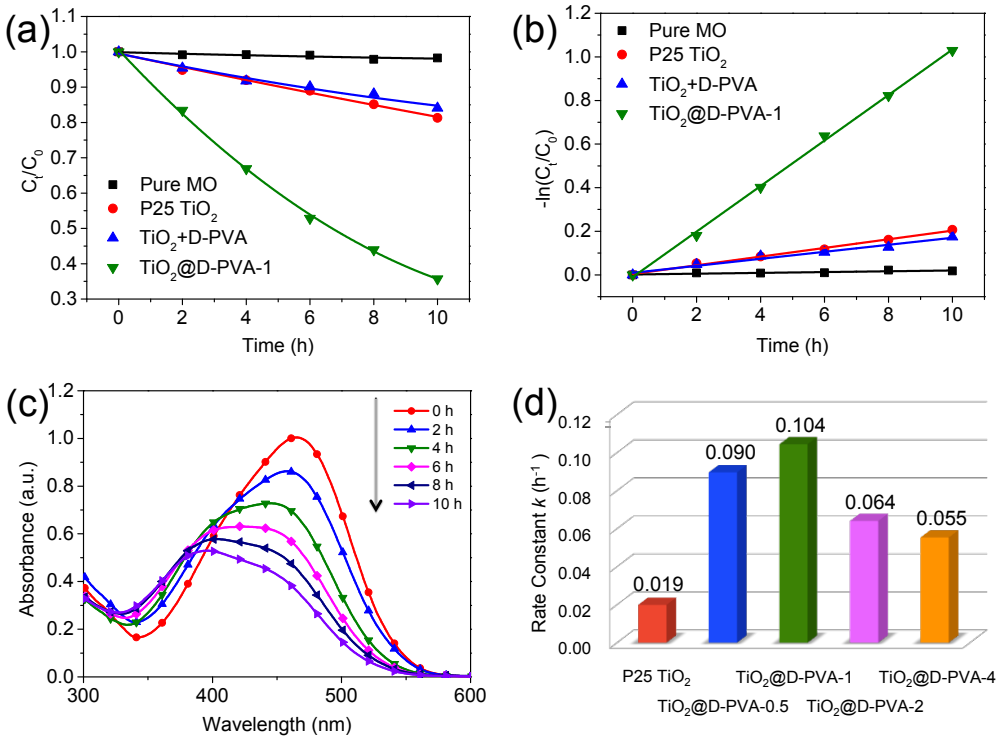

Fig. 7 (a) Photocatalytic degradation of MO by TiO_2@D-PVA-1. (b) Photocatalytic rate constant k of TiO_2@D-PVA-1. (c) UV-vis spectra of MO photocatalyzed by TiO_2@D-PVA-1. (d) Photocatalytic rate constant k of TiO_2@D-PVA samples prepared with different PVA concentration.

Fig. 7(a) demonstrates the photocatalytic activity of TiO_2@D-PVA-1 compared with control samples and Fig. 7(b) demonstrates the first-order fitting of the photocatalytic reaction. It can be observed that under visible light irradiation, MO is very stable in aqueous solution, revealing almost unchanged concentration (k = 0.002 h^{-1}). The P25 TiO_2 sample demonstrates a first-order reaction kinetics of MO degradation (k = 0.019 h^{-1}). Meanwhile, the physical mixture of TiO_2 and D-PVA

(TiO_2+D-PVA) demonstrates a slightly lower photocatalytic activity (k = 0.016 h^{-1}) than that of pure P25. However, the photocatalytic rate constant k of TiO_2@D-PVA-1 is 0.104 h^{-1} which is about 5.5 times higher than that of P25 TiO_2. The marked difference between TiO_2+D-PVA and TiO_2@D-PVA-1 indicates that the interfacial Ti-O-C bonds in TiO_2@D-PVA-1 are beneficial to improve the photocatalytic activity. Thus, it can be inferred that the conjugated D-PVA structures were successfully grafted onto the surface of P25 and the electron transfer pathways were achieved through the interfacial C-O-Ti bonds between TiO_2 and D-PVA [70,72]. The photocatalytic degradation process of MO can be further confirmed as in Fig. 7(c) where the decrease of absorption at 465 nm is visible. The main reason behind the observed blueshift of the maximum absorption wavelength is due to the reactive oxygen radicals (e.g. $\cdot O_2^-$, ·OOH, ·OH) in the bulk solution attack principally at the aromatic ring and end groups (sulfonic group and methyl) [88]. It is reported that the final degradation products of MO are NO_3^-, SO_4^{2-}, CO_2, H_2O, et al. [70].

To further explore the photocatalytic activity of TiO_2@D-PVA, the effect of grafting amount of D-PVA was investigated. As in Fig. 7(d), the grafting amount of D-PVA in the present system can largely affect the MO degradation efficiency. After the grafting of TiO_2 with D-PVA, the photocatalytic rate constant increases gradually with the increase of D-PVA content. The highest photocatalytic rate constant was observed for TiO_2@D-PVA-1. The photocatalytic activity of P25, TiO_2@D-PVA-0.5, TiO_2@D-PVA-1, TiO_2@D-PVA-2, and TiO_2@D-PVA-4 is 0.019 h^{-1}, 0.090 h^{-1}, 0.104 h^{-1}, 0.064 h^{-1}, and 0.055 h^{-1}, respectively. However, further increasing the grafting amount of D-PVA results in the gradual decrease of the photocatalytic rate constant, which is probably due to the opacity and light scattering of the D-PVA decreasing the absorption of light by TiO_2, and the reduced photocatalytic active sites[76,85,89].

3.3. Mechanism of improved photocatalytic activity

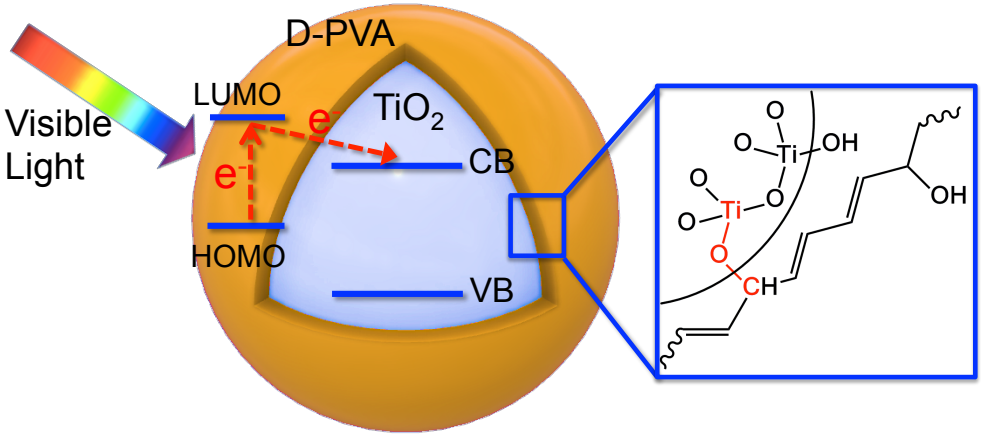

Scheme 1 Schematic representation of possible charge separation and transfer mechanism of TiO_2@D-PVA under visible light irradiation.

Based on our experimental results and previous literatures, the photocatalytic

activity mechanism of TiO_2@D-PVA can be represented by Scheme 1. TiO_2 has a relatively large bandgap of 3.0-3.2 eV, and it cannot absorb visible light [44]. Under high temperature, PVA can form conjugated structures and Ti-O-C bonds through elimination of adjacent hydroxyl groups. The conjugated D-PVA structures can harvest visible light and inject excited electrons into the conduction band (CB) of TiO_2 via Ti-O-C and C=C bonds [69,70,72,74]. Then, the injected electrons subsequently migrate to the edge of TiO_2 and react with the oxygen adsorbed on the surface of TiO_2 to generate reactive oxygen species. The subsequent oxidative and reductive reactions lead to the degradation of the organic pollutants [69,70,72,74].

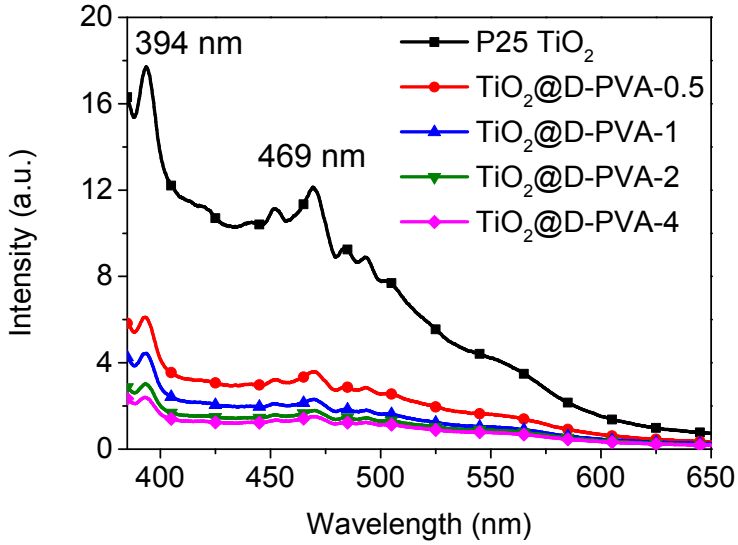

Fig. 8 PL Spectra of P25 and TiO_2@D-PVA

In order to confirm the mechanism stated above, the charge separation and transfer between the TiO_2 and D-PVA was further examined. PL emission spectra is a widely used method for the examination of the recombination rate of electron-hole pairs in semiconductors particles where a lower intensity indicates a lower recombination rate [70,81,90]. As in Fig. 8, the peak observed at 394 nm can be attributed to the bandgap transition in anatase TiO_2 and the peak at 469 nm can be attributed to the transition of oxygen vacancies trapped electrons [70,91,92]. It can be observed that the PL intensity of the synthesized TiO_2@D-PVA demonstrated a significant decrease compared to pure P25 TiO_2, which indicates that the recombination of photogenerated electron-hole pairs has been effectively inhibited via the charge transfer between D-PVA coating and TiO_2 nanoparticles. Thus, the above photocatalytic mechanism of TiO_2@D-PVA is confirmed.

2.4. Conclusion

In summary, a facile and green method to synthesize Degraded-PVA coated TiO_2 (TiO_2@D-PVA) nanoparticles containing conjugated structures was prepared. The TiO_2@D-PVA samples were prepared via physical mixing, centrifugation and calcination, and the actual contents of D-PVA in TiO_2@D-PVA samples demonstrated a positive correlation with the concentration of the PVA solution used.

The photocatalytic degradation activity of the synthesized TiO_2@D-PVA was evaluated by using MO as the model pollutant. The photocatalytic rate constant of TiO_2@D-PVA-1 is about 5.5 times higher than that of P25. The conjugated D-PVA structures can harvest visible light, thus enabling the visible-light photocalytic activity of TiO_2. The interfacial Ti-O-C bonds and the conjugated structures in TiO_2@D-PVA can act as the pathway to quickly transfer the excited electrons between D-PVA and TiO_2, therefore contributing to the increased photocatalytic activity. This facile and green synthesis method of TiO_2@D-PVA may open up a new avenue for fabricating high performance visible light photocatalyst and thus facilitating their practical applications.

3. Facile, green, low-cost, and recyclable polymer dots-grafted TiO_2/ PVA porous composite film for rapid visible light catalyzed degradation of dye pollutants

3.1. Introduction

Today, effluents of a large variety of industries usually contain important quantities of synthetic organic dyes which would cause considerable non-aesthetic pollution and serious health-risk when discharged [28]. The majority of the dye pollutants are complex aromatic compounds with large structural diversity that provides a high degree of chemical, biological and photocatalytic stability and breakdown resistance with time, exposure to sunlight, microorganisms, water, and common cleaning agents [28]. Since conventional wastewater treatment plants cannot degrade the majority of these pollutants, powerful methods for the decontamination of dyes wastewaters have received increasing attention over the past decade [74]. Therefore, a large number of semiconductors have been found to be able to photocatalyze the degradation of various organic contaminants [90,93–96]. Among a large range of possible choices, TiO_2 has been one of the most promising photocatalysts as a clean advanced oxidation technology (AOT) due to its low cost, nontoxicity and long-term stability [71]. However, the main barrier to the effective utilization of its photocatalytic activity is that because of the relatively large bandgap energy of 3.0 to 3.2 eV (anatase), it can only absorb UV-A light under the wavelength of 400 nm, which only takes up less than 4% of the energy from natural sunlight [44]. Therefore, over the past decades, considerable efforts have been directed toward the improvement of the photocatalytic efficiency of TiO_2 in the visible light region [70,72,75,76].

Among these methods, grafting the TiO_2 nanoparticles with semiconductive carbon dots has been proved to be a method with great potential for practical application [70]. As a new type of carbon materials, carbon dots have attracted tremendous attention due to their tuneable photoluminescent (PL) properties, low toxicity, hydrophilic nature, good biocompatibility and excellent photo-stability [97]. Generally, these carbon dots are synthesized through cutting carbonic precursors, such as graphene, graphene oxide, and carbon fiber, into the smaller pieces by chemical oxidation, hydrothermal or solvothermal treatment under harsh conditions which need to use sulfuric acid, nitric acid or other strong oxidizers [97]. These methods usually involve not only high cost and complex fabrication process for the raw materials and complicated post-processing, but also cause potential safety risks and environmental pollution because of the use of strong concentrated acids and the potential generation of toxic gas during the synthesis [97]. Thus, Polymer Dots (PDs), a new class of carbon dots, has been fabricated via a one-step hydrothermal treatment of non-conjugated linear polymers [98]. The PDs consisted of a partial carbonized core wrapped by noncrystalline polymer chains and both parts contributed to the

fluorescent characteristics of the PDs [98]. Thus, PDs made from PolyVinyl Alcohol (PVA) has been successfully grafted on in-situ hydrothermally synthesized TiO_2 nanopartcles by Li *et al.* in a simple two-step method.[70] The synthesized PDs-TiO_2 nanoparticles demonstrated an excellent photocatalytic activity under visible and UV-Vis light and exhibited good recycling stability [70].

Yet another factor that limits the effective practical application of TiO_2 is the difficulty of separation and recycling of the nanoparticles photocatalysts, which may involve tedious and time-consuming steps like filtration or centrifugation [99]. In order to achieve both high photocatalytic performances and easy recover capability, previous researches have immobilized TiO_2 nanoparticles on multiple porous solid structures [40,100–102]. However, most of these substrates are opaque themselves and thus lowers the photocatalytic activity, so a multiple of transparent polymers have been utilized as substrates for loading TiO_2 nanoparticles [103]. As a water-soluble polymer, Polyvinyl alcohol (PVA) is widely used in the fields of fiber, dispersant, glue, and film because of its cheapness and nontoxicity [70]. Thus, it is widely used as functional membranes with high transparency for loading of TiO_2 photocatalysts [103].

In order to realize the visible-light photocatalytic activity of PVA-TiO_2 composite films, previous researches have utilized several different methods. Liu *et al.* have synthesized a transparent PVA/TiO_2 nanocomposite film with trifluoroacetic acid-treated titania xerogel.[103] The film demonstrated an enhanced photocatalytic activity under visible light and good recycling stability.[103] Song *et al.* synthesized a heat-treated PVA/TiO_2 composite film(H-PVA/TiO_2) on a glass slide via combining sol-gel method and heat treatment.[104] The TiO_2 sol was mixed with PVA solution, coated on a glass slide, and finally heat-treated under nitrogen atmosphere.[104] The resulting product demonstrated an effective visible-light photocatalytic activity. [104] By calcinating the film on glass substrates obtained from TiO_2 sol and initially thermally treated PVA solution, Yang *et al*. prepared a Calcinated PVA/TiO_2 composite film with visible-light photocatalytic activity.[86]

However, previous methods used for synthesizing PVA/TiO_2 composite films with visible-light photocatalytic activities in previous studies usually involve several tedious treatment steps with hazardous chemicals while the resulting non-porous film suffers from lower surface area and thus relatively limited photocatalytic activity [86,103,104]. Thus, a facile, low-cost, and green method to synthesize a PVA/TiO_2 composite film with visible-light photocatalytic activity and good recycling stability is of great value with respect to practical application. In this project , we hope to develop a polymer dots-grafted TiO_2/PVA porous composite film (p-PVA/PDs-TiO_2) with visible-light photocatalytic activity and stable recycling properties such that it may be applied in practical use for pollutant degradation in the environment via harvesting energy from sunlight.

3.2. Experimental

3.2.1. Materials

Polyvinyl alcohol (PVA, M_W ~250,000, DS=0.9) was purchased from Acros Organics. Calcium Carbonate ($CaCO_3$, 98%, Heavy Powder FCC) was purchased from Spectrum Chemical MFG Corp. Hydrochloric acid (HCl, 1 wt%) was purchased from Flinn. Scientific. TiO_2 (P25, 20% rutile and 80% anatase) with a mean diameter of 21 nm was provided by Evonik Industries, Germany. Methyl orange (MO), used as the model pollutant, was manufactured by Zhejiang Yongjia Fine Chemical Plant, China. All chemicals were used without further purification.

3.2.2. Synthesis of PDs-TiO_2

4 g PVA was mixed with 396 mL deionized water in a 500 mL round flask under continuously stirring for 3 h at 95 °C, the obtained PVA solution was colorless and transparent. Then 70 g of the PVA solution was transferred to a 100 mL Teflon autoclave. After reaction at 200 °C for 7 h, the reactor was cooled down to room temperature naturally. PDs solution and 2 g $Ti(SO_4)_2$ was mixed with 56 g deionized water in a 100 mL Teflon autoclave, and 2 g sulfuric acid was added dropwise into the autoclave under continuously stirring. The mixture was kept stirring for 30 min at room temperature to obtain a transparent solution. After reaction at 200 °C for 7 h, the autoclave was cooled down to room temperature naturally. The resulting PDs-TiO_2 nanohybrids were collected by centrifugation and then washed with deionized water until no $SO_4^{2-}$was detected by 0.5 mol/L $BaCl_2$ solution. Finally the nanohybrids were dried under vacuum at 100 °C overnight.

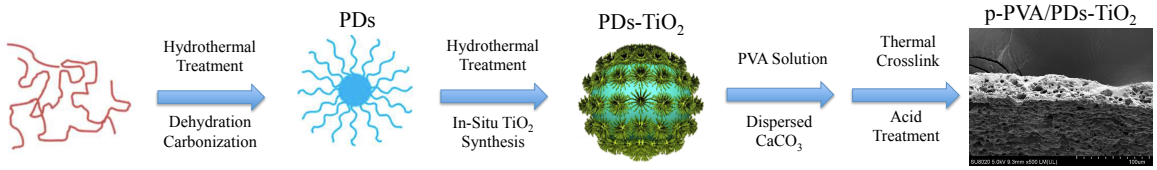

Scheme 2. General procedure for the synthesis of p-PVA/PDs-TiO_2

3.2.3. Synthesis of p-PVA/PDs-TiO_2

The general procedure for the synthesis of p-PVA/PDs-TiO_2 is outlined as in Scheme 2.15 g of PVA is mixed with 185 mL of DI water and is mechanically stirred for 1h (300 rpm). The solution is then heated to 95 °C for 3 h and a 7.5 wt% solution is obtained. PDs-TiO_2 nanoparticles containing 150 mg of TiO_2 are ultrasonically dispersed for 2 minutes in 7.5 mL of DI water. 20 g of 7.5 wt% PVA solution is then added to the solution and the solution is stirred for 15 min. 0.75 g of $CaCO_3$ is mixed with 5 mL of DI water, dispersed ultrasonically, and then added to the PVA-TiO_2 solution. The solution is then stirred for 30 min to obtain the PVA/PDs-TiO_2/$CaCO_3$ solution. The PVA-TiO_2-$CaCO_3$ solution is then spread onto a glass panel into a film with thickness of 1 mm. After the film has dried under room temperature, it is heat-treated at 130 °C for 3 h to yield the cross-linked PVA/PDs-TiO_2/$CaCO_3$ film. The film is then transferred to 300 mL of 1 wt% HCl solution and is immersed for 30 min. The film is then washed for 6 times with DI water and is marked as the porous PVA/PDs-TiO_2 film (p-PVA/PDs-TiO_2).

3.2.4. Characterization

The morphology of the PVA/TiO_2 and p-PVA/ TiO_2 is characterized by ascanning electron microscope (SEM, SU8020, Hitachi) respectively. Thermogravimetric Analysis (TGA) of the p-PVA/PDs-TiO_2 and PDs-TiO_2 is conducted on a Thermogravimetric Analyzer (TGA, TGA8000, Perkin-Elmer). The Fourier-Transform Infrared Spectroscopy (FTIR/ATR, Nicolet iS5 with iD7 ATR module, Thermo Scientific) are of the PDs-TiO_2 and p-PVA/PDs-TiO_2 also conducted. Photoluminescence (PL) of PDs-TiO_2 measurements were performed at room temperature with a Shimadzu RF-6000 fluorescence spectrometer.

3.2.5. Photocatalytic Degradation

The photocatalytic activity of the synthesized PDs-TiO_2 awas evaluated via the degradation rate of MO solution of 15 mg/L. 20 mL of the MO solution was mixed with the sample containing 40 mg TiO_2 in a 30 mL container. Prior to visible light irradiation, the sample was ultrasonically dispersed and was placed in dark under magnetic stirring for 1 h to achieve adsorption-desorption equilibrium. The light source was a 300 W halogen lamp (SF-300C, ScienceTech Inc.) equipped with an ultraviolet cut off filter (λ> 400 nm). The lamp was put in a cylindrical glass vessel with a recycling water glass jacket to make sure that the mixed solution was kept at room temperature. At regular time intervals, a 5 mL solution was examined by measuring the absorption at 465 nm using an UV-Vis spectrophotometer (UV-2700, Shimadzu). The process above is also repeated with a AM1.5G simulated sunlight filter instead of a UV cutoff filter to examine the photocatalytic activity of the p-PVA/PDs-TiO_2 film under sunlight spectrum. MO degradation efficiency was calculated by the ratio of concentration (C_t/C_0, C_t, and C_0 can be calculated by the absorbance intensity).

3.3. Results and Discussion

3.3.1. Characterization of PDs-TiO_2

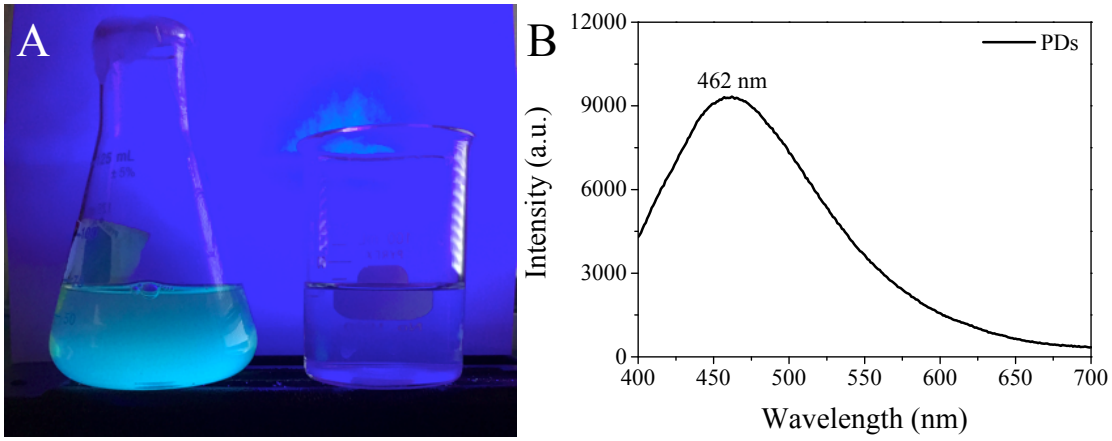

Fig. 9. A) Photograph and B) PL Spectrum of PDs under 365 nm UV Light Irradiation

One unique advantage of carbon dots is their fluorescence emission property. Fig. 9A shows that the PDs aqueous solution could emit bright cyan fluorescence under 365 nm UV light irradiation at wavelength of 462 nm as shown in Fig. 9B, which is in good agreement with previous literature [70].

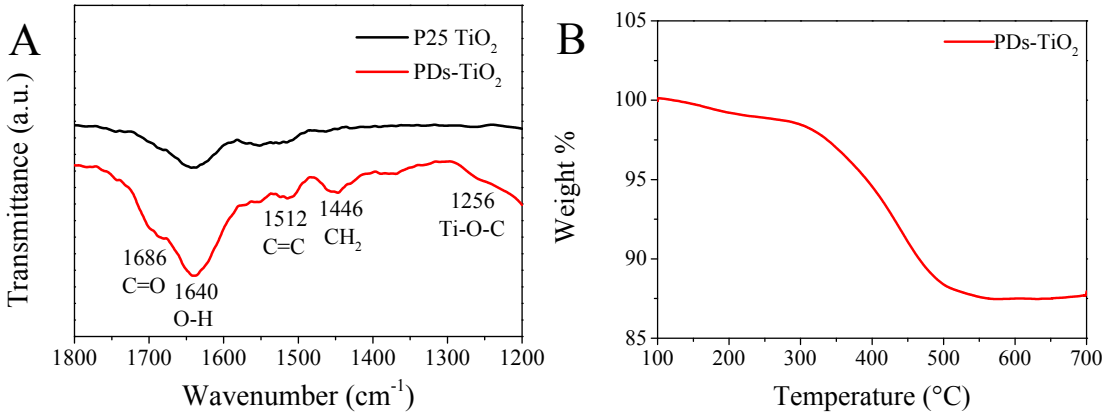

Fig. 10. A) FT-IR Spectrum and B) TGA of PDs-TiO_2 nanoparticles

FT-IR spectrum was used to investigate the interaction between the PDs and TiO_2 nanoparticles as in Fig. 10A. For P25 TiO_2, the peak at 1640 cm^{-1} corresponding to the physically adsorbed water and surface hydroxyl groups is observed [70]. Compared with TiO_2, several new peaks appearing at 1686, 1512, and 1446 cm^{-1} in PDs-TiO_2 are attributed to C=O stretching, C=C stretching and CH_2 bending vibration absorption respectively, suggesting that the presence of conjugated structures in the PDs in the PDs-TiO_2 nanoparticles [70,72,86,104,105]. In particular, the very peak at 1256 cm^{-1} may be ascribed to the Ti-O-C bonds vibration absorption, indicating that PDs are chemically grafted on the surface of TiO_2 nanoparticles in the PDs-TiO_2 [70,72,105]. TGA was used to investigate the actual loading content of PDs in PDs-TiO_2. As shown in Fig. 10B, the loading content of PDs in PDs-TiO_2 is about 11.27 wt% as indicated by the weight loss between about 300 °C to 500 °C while the initial weight loss of about 1.21 wt% between 100 °C to 300 °C can be attributed to physically adsorbed water.

3.3.2. Characterization of p-PVA/PDs-TiO_2

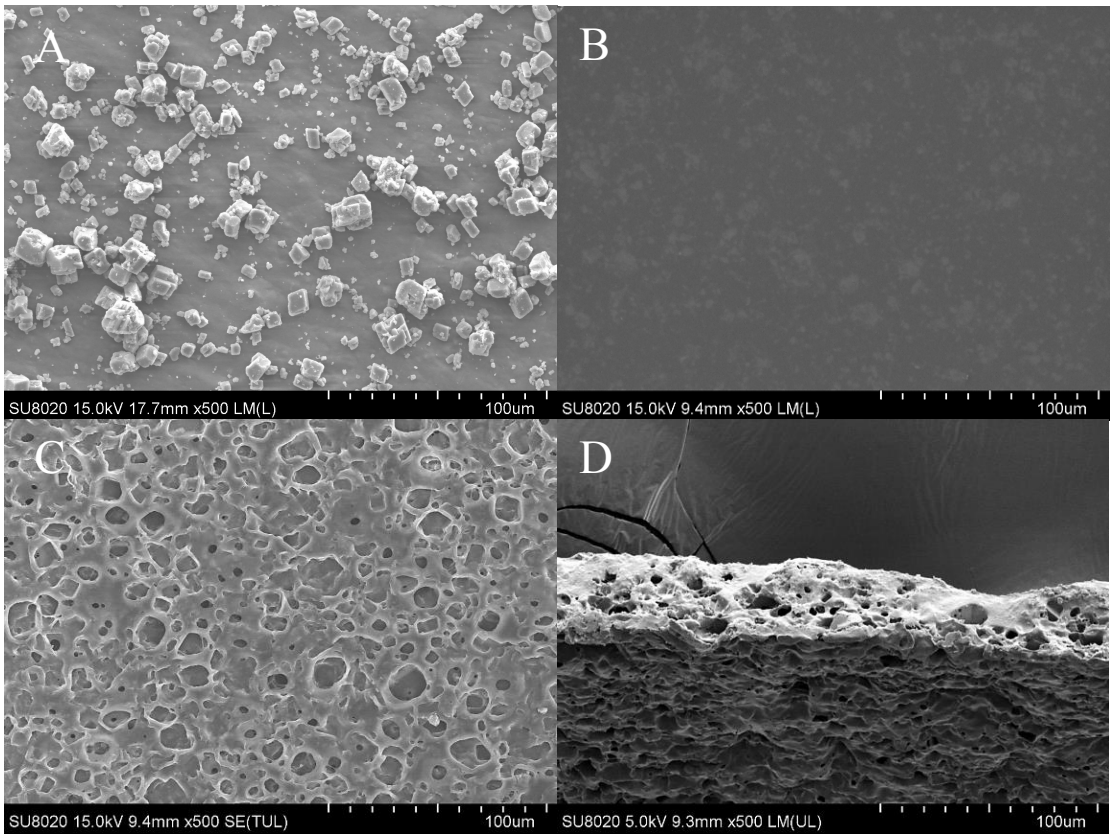

Fig. 11. SEM image of A) $CaCO_3$ particles B) PVA/P25 TiO_2 composite film C, D) p-PVA/P25 TiO_2 composite film

SEM was used to investigate the surface morphology of the p-PVA/P25 TiO_2 composite film. As shown in Fig. 11A, the $CaCO_3$ used in the synthesis consists of microscale-sized particles with size distributed approximately between 5 μm to 15 μm. In contrast to the PVA/P25 TiO_2 composite film which has a smooth surface as shown in Fig. 11B, the surface of p-PVA/P25 TiO_2 composite film is porous as shown in Fig. 11C. The size of the pores is distributed approximately between 5 μm to 20 μm, which is in good agreement with the size of the $CaCO_3$ particles, proving the microscale pores have been successfully introduced into the p-PVA/P25 TiO_2 composite film through the dissolution of the $CaCO_3$ particles. In addition to the increased in the surface area of the film, which accelerates the contact between the dye pollutants and the nanoparticles, small white areas with the size of about 10 μm observed in the PVA/P25 TiO_2 composite film is no longer observed in the p-PVA/P25 TiO_2 composite film. These white areas can be attributed to the aggregation of the TiO_2 nanoparticles in the PVA substrate, and through reducing the physical aggregation, the photocatalytic activity of the p-PVA/P25 TiO_2 composite film can also be improved [105].

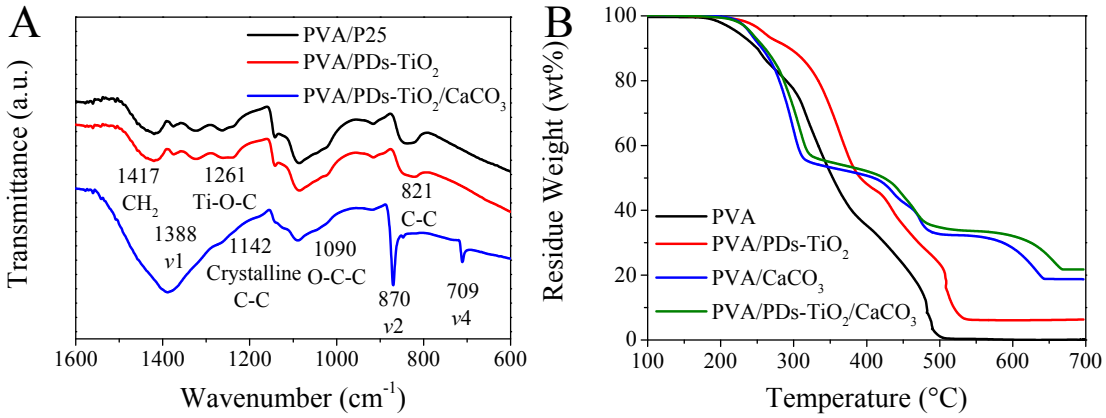

Fig. 12. A) FT-IR Spectrum and B) TGA of PVA/P25, PVA/PDs-TiO_2, and PVA/PDs-TiO_2/$CaCO_3$

FT-IR spectrum was also used to investigate the interaction between the PDs-TiO_2 nanoparticles and the PVA substrate as in Fig. 12A. For PVA/P25 TiO_2 and PVA/PDs-TiO_2, the peak appearing at 1417 cm^{-1} and 1142 cm^{-1} is attributed to CH_2 bending vibrations and the C-C stretching vibration in the crystalline regions in the PVA substrate as the PVA chains absorb heat and rearranged formed during the heat treatment [105]. The other peaks at 1090 cm^{-1} and 821 cm^{-1} are attributed to the O-C-C bonds sand C-C bonds in the PVA substrate [105]. In addition, the absorption peak at 1261 cm^{-1} corresponding to the Ti-O-C bond vibration is present in both PVA/P25 TiO_2 and PVA/PDs-TiO_2, which indicates that the Ti-O-C bond observed here corresponds to the Ti-O-C bond formed between the PVA substrate and the surface hydroxyl groups of the TiO_2 nanoparticles, confirming that the nanoparticles are chemically immobilized in the substrate [105]. In the FT-IR spectrum of PVA/PDs-TiO_2/$CaCO_3$, three very strong peaks at 1388 cm^{-1}, 870 cm^{-1}, and 709 cm^{-1} corresponding to the ν1 symmetric stretching, ν2 out-of-plane bending, and ν4 in-plane bending vibrations of the carbonate ions in $CaCO_3$ are observed, confirming the embedding of $CaCO_3$ particles in PVA/PDs-TiO_2/$CaCO_3$, which are then treated with acid to dissolve the $CaCO_3$ particles to create the desired microscale porosity [106]. TGA was used to investigate the actual loading content of in PDs-TiO_2 and $CaCO_3$ in PVA/PDs-TiO_2/$CaCO_3$ composite film. As shown in Fig. 12B, pure PVA substrate can be completely degraded at about 500 °C. In comparison, the loading content of TiO_2 in the PVA/PDs-TiO_2 is approximately 6.09 wt%. In addition, while the loading content of pure PVA/$CaCO_3$ control film sample is approximately 18.80 wt%, the loading content of TiO_2 in PVA/PDs-TiO_2/$CaCO_3$ composite film is approximately 2.99 wt%. Taking the increased total weight due to the presence of $CaCO_3$ in the film into account, the two values agree well among themselves.

3.3.3. Photocatalytic Activity

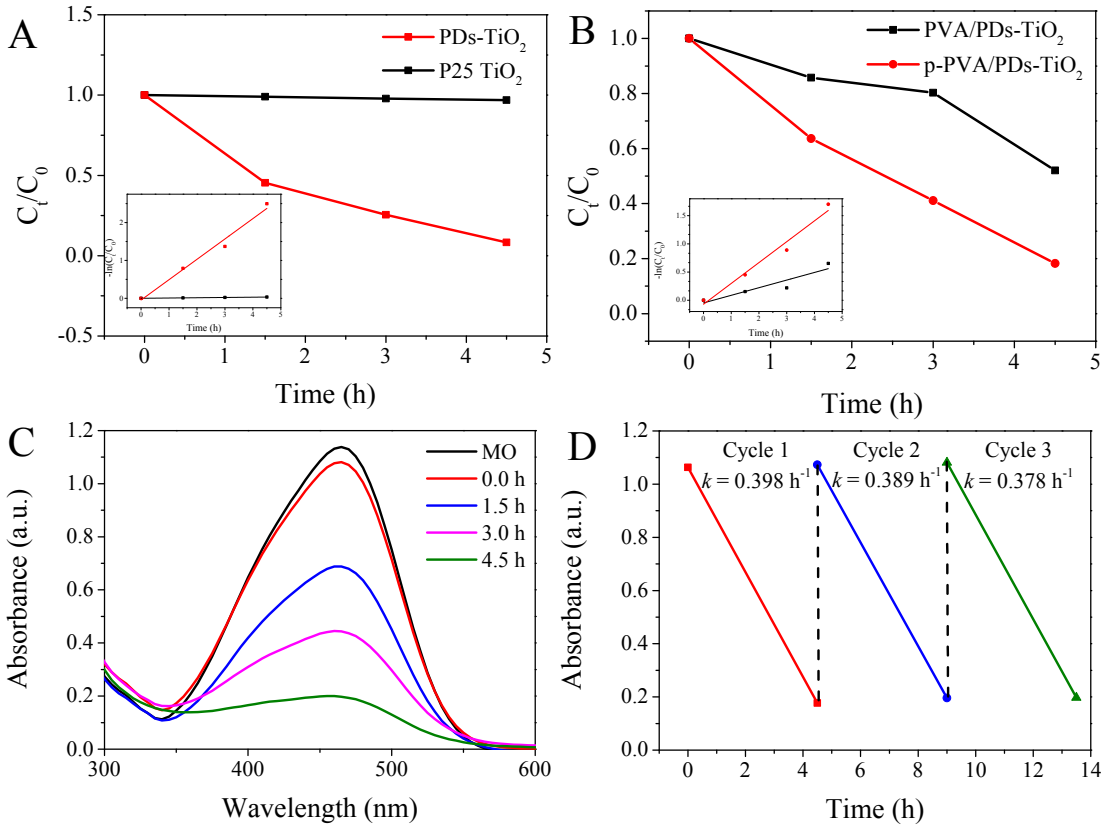

Fig. 13. A) Photocatalytic Degradation of MO by PDs-TiO_2 and P25 TiO_2 under visible light (inset: photocatalytic rate constant *k*) B) Photocatalytic Degradation of MO by PVA/PDs-TiO_2 and p-PVA/PDs-TiO_2 under AM1.5G simulated sunlight C) UV-Vis spectra of MO Degradation catalyzed with p-PVA/PDs-TiO_2 (inset: photocatalytic rate constant *k*) D) Recycle photocatalytic performance test of with p-PVA/PDs-TiO_2 under AM1.5G simulated sunlight

Fig. 13A demonstrates the visible-light photocatalytic activity of PDs-TiO_2 compared with unmodified P25 TiO_2 samples and the inset demonstrates the first-order fitting of the photocatalytic reaction. It can be observed that the P25 TiO_2 sample demonstrates a first-order reaction kinetics of MO degradation (k = 0.007 h^{-1}). However, the photocatalytic rate constant k of PDs-TiO_2 is 0.538 h^{-1} which is about 76.9 times higher than that of P25 TiO_2. The marked difference between PDs-TiO_2 and P25 TiO_2 indicates that the interfacial Ti-O-C bonds in PDs-TiO_2 are essential to improving the visible-light photocatalytic activity [70]. For practical application, photocatalyst is always expected to be useful for a relatively long time under UV-Vis light irradiation [70]. Thus, the photocatalytic activity and recyclability of the p-PVA/PDs-TiO_2 sample was measured under AM1.5G simulated sunlight. Fig. 13B demonstrates the photocatalytic activity of p-PVA/PDs-TiO_2 compared with the nonporous PVA/PDs-TiO_2 under AM1.5G simulated sunlight. As shown in the inset, the degradation also follows a first-order kinetics, with the rate constant of the porous p-PVA/PDs-TiO_2 sample (k = 0.370 h^{-1}) being approximately 2.74 times of that of the nonporous PVA/PDs-TiO_2 sample (k = 0.135 h^{-1}). The photocatalytic degradation process of MO can be further confirmed as in Fig. 13C where the decrease of

absorption at 465 nm is visible. The main reason behind the observed blueshift of the maximum absorption wavelength is due to the reactive oxygen radicals (e.g. $\cdot O_2^-$, ·OOH, ·OH) in the bulk solution attack principally at the aromatic ring and end groups (sulfonic group and methyl) [88]. It is reported that the final degradation products of MO are NO_3^-, SO_4^{2-}, CO_2, H_2O, et al. [70]. As shown Fig. 13D, the p-PVA/PDs-TiO_2 sample exhibits good recycle stability under AM1.5G simulated sunlight irradiation, with the rate constant decreasing by only 5.03%.

3.4. Conclusion

In summary, a Porous PVA Film Loaded with Polymer Dots-grafted TiO_2 Nanoparticles (p-PVA/PDs-TiO_2) is synthesized with a facile, green, and low-cost method. The hydrothermally synthesized PDs are grafted on TiO_2 nanoparticles in-situ via a second hydrothermal treatment. The PDs-TiO_2 are then mixed with PVA and $CaCO_3$ particles for solution casting, which is then thermally crosslinked and treated with dilute acid to dissolve the $CaCO_3$ particles and create a porous p-PVA/PDs-TiO_2. The pore size is approximately between 5 μm to 20 μm and the loading content of PDs-TiO_2 is approximately 6.09 % in the final p-PVA/PDs-TiO_2 composite film. The photocatalytic rate of PDs-TiO_2 under visible light is about 76.9 times higher than commercial TiO_2 nanoparticles. The photocatalytic rate of p-PVA/PDs-TiO_2 under sunlight is about 2.74 times higher than the nonporous sample. The composite film demonstrated an excellent stability after 3 cycles of 4.5 h each of simulated sunlight, with the rate constant decreasing by only approximately 5%. This novel p-PVA/PDs-TiO_2 film is a promising method to prepare polymer/TiO_2 hybrid material with high photocatalytic activity under visible light for multi-cycle use, which is of significance to the application of TiO_2 catalysts in wastewater treatment industry.

4. Summary of Results

Synthesizing polymer nanocomposites have been proved to be one of the most promising directions for enhancing the photocatalytic performance of TiO_2 nanoparticles for real-life applications. The photocatalytic activity is improved through grafting of conjugated polymers and the recycling stability is enhanced through loading in polymer matrices. In addition, the process of synthesizing such composites are improved and simplified under the guidelines of green chemistry, which is crucial for practical application and industrialization in the future. The main accomplishments of this research are as listed below.

1. A facile and green method to synthesize Degraded-PVA coated TiO_2 (TiO_2@D-PVA) nanoparticles containing conjugated structures was prepared via physical mixing, centrifugation, and calcination. The content of D-PVA in TiO_2@D-PVA is optimized through controlling the concentration of the PVA solution, and the optimal concentration is determined to be 5 wt%. Further mechanism study confirms that the Ti-O-C interfacial bonds and the conjugated structures in D-PVA could facilitate the electron transfer between D-PVA and TiO_2, thus contributing to the enhanced visible light photocatalytic activity.
2. A polymer dots-grafted TiO_2/PVA porous composite film (p-PVA/PDs-TiO_2) was synthesized through immobilizing polymer dots grafted TiO_2 (PDs-TiO_2) nanoparticles synthesized via a two-step hydrothermal reaction onto a PVA film. Through introducing microscale porosity by means of dissolving $CaCO_3$ particles introduced during solution casting, the sunlight photocatalytic activity of the porous TiO_2/PVA porous composite film is approximately 2.74 times higher than the nonporous sample. In addition, the composite film demonstrated excellent stability after 3 cycles of 4.5 h each of AM 1.5 G simulated sunlight, with the rate constant decreasing by only approximately 5%.

References

[1] S.M. Gupta, M. Tripathi, A review of TiO_2 nanoparticles, Chinese Sci. Bull. 56 (2011) 1639. doi:10.1007/s11434-011-4476-1.

[2] M. Choi, J. Lim, M. Baek, W. Choi, W. Kim, K. Yong, Investigating the Unrevealed Photocatalytic Activity and Stability of Nanostructured Brookite TiO_2 Film as an Environmental Photocatalyst, ACS Appl. Mater. Interfaces. 9 (2017) 16252–16260. doi:10.1021/acsami.7b03481.

[3] A. Sclafani, L. Palmisano, M. Schiavello, Influence of the preparation methods of titanium dioxide on the photocatalytic degradation of phenol in aqueous dispersion, J. Phys. Chem. 94 (1990) 829–832. doi:10.1021/j100365a058.

[4] J. Muscat, V. Swamy, N.M. Harrison, First-principles calculations of the phase stability of TiO_2, Phys. Rev. B. 65 (2002) 224112. doi:10.1103/PhysRevB.65.224112.

[5] O. Carp, C.L. Huisman, A. Reller, Photoinduced reactivity of titanium dioxide, Prog. Solid State Chem. 32 (2004) 33–177. doi:https://doi.org/10.1016/j.progsolidstchem.2004.08.001.

[6] H. Zhang, J. F. Banfield, Thermodynamic analysis of phase stability of nanocrystalline titania, J. Mater. Chem. 8 (1998) 2073–2076. doi:10.1039/A802619J.

[7] H. Zhang, J.F. Banfield, Understanding Polymorphic Phase Transformation Behavior during Growth of Nanocrystalline Aggregates: Insights from TiO_2, J. Phys. Chem. B. 104 (2000) 3481–3487. doi:10.1021/jp000499j.

[8] K. Tanaka, M.F. V Capule, T. Hisanaga, Effect of crystallinity of TiO_2 on its photocatalytic action, Chem. Phys. Lett. 187 (1991) 73–76. doi:https://doi.org/10.1016/0009-2614(91)90486-S.

[9] A. Selloni, Anatase shows its reactive side, Nat. Mater. 7 (2008) 613. https://doi.org/10.1038/nmat2241.

[10] S.K. Poznyak, A.I. Kokorin, A.I. Kulak, Effect of electron and hole acceptors on the photoelectrochemical behaviour of nanocrystalline microporous TiO_2 electrodes, J. Electroanal. Chem. 442 (1998) 99–105. doi:https://doi.org/10.1016/S0022-0728(97)00458-0.

[11] F. Pedraza, A. Vazquez, Obtention of TiO_2 rutile at room temperature through direct Oxidation of TiCl3, J. Phys. Chem. Solids. 60 (1999) 445–448. doi:https://doi.org/10.1016/S0022-3697(98)00315-1.

[12] Y. Xie, C. Yuan, Characterization and photocatalysis of Eu^{3+}–TiO2 sol in the hydrosol reaction system, Mater. Res. Bull. 39 (2004) 533–543. doi:https://doi.org/10.1016/j.materresbull.2004.01.001.

[13] S. Yin, Y. Fujishiro, J. Wu, M. Aki, T. Sato, Synthesis and photocatalytic properties of fibrous titania by solvothermal reactions, J. Mater. Process. Technol. 137 (2003) 45–48. doi:https://doi.org/10.1016/S0924-0136(02)01065-8.

[14] M. Hirano, C. Nakahara, K. Ota, O. Tanaike, M. Inagaki, Photoactivity and

phase stability of ZrO_2-doped anatase-type TiO_2 directly formed as nanometer-sized particles by hydrolysis under hydrothermal conditions, J. Solid State Chem. 170 (2003) 39–47. doi:https://doi.org/10.1016/S0022-4596(02)00013-0.

[15] Q. Zhang, L. Gao, Preparation of Oxide Nanocrystals with Tunable Morphologies by the Moderate Hydrothermal Method: Insights from Rutile TiO2, Langmuir. 19 (2003) 967–971. doi:10.1021/la020310q.

[16] H. Okudera, Y. Yokogawa, Fabrication of titania-coated silica fibers and effect of substrate shape on coating growth rate, Thin Solid Films. 423 (2003) 119–124. doi:https://doi.org/10.1016/S0040-6090(02)01039-8.

[17] A.R. Phani, S. Santucci, Structural characterization of iron titanium oxide synthesized by sol–gel spin-coating technique, Mater. Lett. 50 (2001) 240–245. doi:https://doi.org/10.1016/S0167-577X(01)00232-4.

[18] P. Yang, C. Lu, N. Hua, Y. Du, Titanium dioxide nanoparticles co-doped with Fe^{3+} and Eu^{3+} ions for photocatalysis, Mater. Lett. 57 (2002) 794–801. doi:https://doi.org/10.1016/S0167-577X(02)00875-3.

[19] A.C. Jones, P.R. Chalker, Some recent developments in the chemical vapour deposition of electroceramic oxides, J. Phys. D. Appl. Phys. 36 (2003) R53–R79. doi:10.1088/0022-3727/36/6/202.

[20] R. Van de Krol, A. Goossens, J. Schoonman, Mott-Schottky Analysis of Nanometer-Scale Thin-Film Anatase TiO_2, J. Electrochem. Soc. 144 (1997) 1723–1727. doi:10.1149/1.1837668.

[21] P.P. Ahonen, E.I. Kauppinen, J.C. Joubert, J.L. Deschanvres, G. Van Tendeloo, Preparation of nanocrystalline titania powder via aerosol pyrolysis of titanium tetrabutoxide, J. Mater. Res. 14 (1999) 3938–3948. doi:DOI: 10.1557/JMR.1999.0533.

[22] J. Zhao, M. Milanova, M.M.C.G. Warmoeskerken, V. Dutschk, Surface modification of TiO_2 nanoparticles with silane coupling agents, Colloids Surfaces A Physicochem. Eng. Asp. 413 (2012) 273–279. doi:https://doi.org/10.1016/j.colsurfa.2011.11.033.

[23] X. Lu, X. Lv, Z. Sun, Y. Zheng, Nanocomposites of poly(l-lactide) and surface-grafted TiO_2 nanoparticles: Synthesis and characterization, Eur. Polym. J. 44 (2008) 2476–2481. doi:https://doi.org/10.1016/j.eurpolymj.2008.06.002.

[24] Y. Lou, M. Liu, X. Miao, L. Zhang, X. Wang, Improvement of the mechanical properties of nano- TiO_2/poly(vinyl alcohol) composites by enhanced interaction between nanofiller and matrix, Polym. Compos. 31 (2010) 1184–1193. doi:10.1002/pc.20905.

[25] A.T. Paxton, L. Thiên-Nga, Electronic structure of reduced titanium dioxide, Phys. Rev. B. 57 (1998) 1579–1584. doi:10.1103/PhysRevB.57.1579.

[26] J.H. Carey, J. Lawrence, H.M. Tosine, Photodechlorination of PCB's in the presence of titanium dioxide in aqueous suspensions, Bull. Environ. Contam. Toxicol. 16 (1976) 697–701. doi:10.1007/BF01685575.

[27] A. Heller, Chemistry and Applications of Photocatalytic Oxidation of Thin Organic Films, Acc. Chem. Res. 28 (1995) 503–508.

doi:10.1021/ar00060a006.
[28] C.A. Martínez-Huitle, E. Brillas, Decontamination of wastewaters containing synthetic organic dyes by electrochemical methods: A general review, Appl. Catal. B Environ. 87 (2009) 105–145. doi:10.1016/j.apcatb.2008.09.017.
[29] E. Brillas, C.A. Martínez-Huitle, Decontamination of wastewaters containing synthetic organic dyes by electrochemical methods. An updated review, Appl. Catal. B Environ. 166 (2015) 603–643. doi:https://doi.org/10.1016/j.apcatb.2014.11.016.
[30] G.A. Epling, C. Lin, Photoassisted bleaching of dyes utilizing TiO_2 and visible light, Chemosphere. 46 (2002) 561–570. doi:https://doi.org/10.1016/S0045-6535(01)00173-4.
[31] D. Sud, P. Kaur, Heterogeneous Photocatalytic Degradation of Selected Organophosphate Pesticides: A Review, Crit. Rev. Environ. Sci. Technol. 42 (2012) 2365–2407. doi:10.1080/10643389.2011.574184.
[32] G.R.M. Echavia, F. Matzusawa, N. Negishi, Photocatalytic degradation of organophosphate and phosphonoglycine pesticides using TiO_2 immobilized on silica gel, Chemosphere. 76 (2009) 595–600. doi:https://doi.org/10.1016/j.chemosphere.2009.04.055.
[33] I.K. Konstantinou, T.M. Sakellarides, V.A. Sakkas, T.A. Albanis, Photocatalytic Degradation of Selected s-Triazine Herbicides and Organophosphorus Insecticides over Aqueous TiO_2 Suspensions, Environ. Sci. Technol. 35 (2001) 398–405. doi:10.1021/es001271c.
[34] S. Parra, J. Olivero, C. Pulgarin, Relationships between physicochemical properties and photoreactivity of four biorecalcitrant phenylurea herbicides in aqueous TiO_2 suspension, Appl. Catal. B Environ. 36 (2002) 75–85. doi:https://doi.org/10.1016/S0926-3373(01)00283-1.
[35] E. Vulliet, C. Emmelin, J.-M. Chovelon, C. Guillard, J.-M. Herrmann, Photocatalytic degradation of sulfonylurea herbicides in aqueous TiO_2, Appl. Catal. B Environ. 38 (2002) 127–137. doi:https://doi.org/10.1016/S0926-3373(02)00035-8.
[36] X. Meng, Z. Qian, H. Wang, X. Gao, S. Zhang, M. Yang, Sol–gel immobilization of SiO2/TiO2 on hydrophobic clay and its removal of methyl orange from water, J. Sol-Gel Sci. Technol. 46 (2008) 195–200. doi:10.1007/s10971-008-1677-4.
[37] N. Kieda, T. Tokuhisa, Immobilization of TiO_2 Photocatalyst Particles on Stainless Steel Substrates by Electrolytically Deposited Pd and Cu, J. Ceram. Soc. Japan. 114 (2006) 42–45. doi:10.2109/jcersj.114.42.
[38] S. Matsuzawa, C. Maneerat, Y. Hayata, T. Hirakawa, N. Negishi, T. Sano, Immobilization of TiO_2 nanoparticles on polymeric substrates by using electrostatic interaction in the aqueous phase, Appl. Catal. B Environ. 83 (2008) 39–45. doi:https://doi.org/10.1016/j.apcatb.2008.01.036.
[39] S.N. Hosseini, S.M. Borghei, M. Vossoughi, N. Taghavinia, Immobilization of TiO_2 on perlite granules for photocatalytic degradation of phenol, Appl. Catal. B Environ. 74 (2007) 53–62. doi:https://doi.org/10.1016/j.apcatb.2006.12.015.

[40] J. Zhang, H. Yang, L. Jiang, Y. Dan, Enhanced photo-catalytic activity of the composite of TiO_2 conjugated derivative of polyvinyl alcohol immobilized on cordierite under visible light irradiation, J. Energy Chem. 25 (2016) 55–61. doi:10.1016/j.jechem.2015.10.010.

[41] A. Fernández, G. Lassaletta, V.M. Jiménez, A. Justo, A.R. González-Elipe, J.-M. Herrmann, H. Tahiri, Y. Ait-Ichou, Preparation and characterization of TiO_2 photocatalysts supported on various rigid supports (glass, quartz and stainless steel). Comparative studies of photocatalytic activity in water purification, Appl. Catal. B Environ. 7 (1995) 49–63. doi:https://doi.org/10.1016/0926-3373(95)00026-7.

[42] J. Zeng, S. Liu, J. Cai, L. Zhang, TiO_2 Immobilized in Cellulose Matrix for Photocatalytic Degradation of Phenol under Weak UV Light Irradiation, J. Phys. Chem. C. 114 (2010) 7806–7811. doi:10.1021/jp1005617.

[43] S. Yao, J. Li, Z. Shi, Immobilization of TiO_2 nanoparticles on activated carbon fiber and its photodegradation performance for organic pollutants, Particuology. 8 (2010) 272–278. doi:https://doi.org/10.1016/j.partic.2010.03.013.

[44] R. Miao, Z. Luo, W. Zhong, S.Y. Chen, T. Jiang, B. Dutta, Y. Nasr, Y. Zhang, S.L. Suib, Mesoporous TiO_2 with carbon quantum dots as a high-performance visible light photocatalyst, Appl. Catal. B Environ. 189 (2016) 26–38. doi:10.1016/j.apcatb.2016.01.070.

[45] W. Choi, A. Termin, M.R. Hoffmann, The Role of Metal Ion Dopants in Quantum-Sized TiO_2: Correlation between Photoreactivity and Charge Carrier Recombination Dynamics, J. Phys. Chem. 98 (1994) 13669–13679. doi:10.1021/j100102a038.

[46] A.V. Rupa, D. Divakar, T. Sivakumar, Titania and Noble Metals Deposited Titania Catalysts in the Photodegradation of Tartazine, Catal. Letters. 132 (2009) 259–267. doi:10.1007/s10562-009-0108-7.

[47] J. Papp, H.S. Shen, R. Kershaw, K. Dwight, A. Wold, Titanium(IV) oxide photocatalysts with palladium, Chem. Mater. 5 (1993) 284–288. doi:10.1021/cm00027a009.

[48] W.K. Wong, M.A. Malati, Doped TiO_2 for solar energy applications, Sol. Energy. 36 (1986) 163–168. doi:https://doi.org/10.1016/0038-092X(86)90122-2.

[49] N.-L. Wu, M.-S. Lee, Enhanced TiO_2 photocatalysis by Cu in hydrogen production from aqueous methanol solution, Int. J. Hydrogen Energy. 29 (2004) 1601–1605. doi:https://doi.org/10.1016/j.ijhydene.2004.02.013.

[50] R. Asahi, T. Morikawa, T. Ohwaki, K. Aoki, Y. Taga, Visible-Light Photocatalysis in Nitrogen-Doped Titanium Oxides, Science (80-.). 293 (2001) 269 LP – 271. doi:10.1126/science.1061051.

[51] J.C. Yu, Yu, Ho, Jiang, Zhang, Effects of F- Doping on the Photocatalytic Activity and Microstructures of Nanocrystalline TiO_2 Powders, Chem. Mater. 14 (2002) 3808–3816. doi:10.1021/cm020027c.

[52] S. Sakthivel, H. Kisch, Daylight Photocatalysis by Carbon-Modified Titanium Dioxide, Angew. Chemie Int. Ed. 42 (2003) 4908–4911.

doi:10.1002/anie.200351577.

[53] E. Abraham, D. Kam, Y. Nevo, R. Slattegard, A. Rivkin, S. Lapidot, O. Shoseyov, Highly Modified Cellulose Nanocrystals and Formation of Epoxy-Nanocrystalline Cellulose (CNC) Nanocomposites, ACS Appl. Mater. Interfaces. 8 (2016) 28086–28095. doi:10.1021/acsami.6b09852.

[54] B. Patrick, P. V Kamat, Photoelectrochemistry in semiconductor particulate systems. 17. Photosensitization of large-bandgap semiconductors: charge injection from triplet excited thionine into zinc oxide colloids, J. Phys. Chem. 96 (1992) 1423–1428. doi:10.1021/j100182a072.

[55] P. V Kamat, Photochemistry on nonreactive and reactive (semiconductor) surfaces, Chem. Rev. 93 (1993) 267–300. doi:10.1021/cr00017a013.

[56] J.C. Yu, Y. Xie, H.Y. Tang, L. Zhang, H.C. Chan, J. Zhao, Visible light-assisted bactericidal effect of metalphthalocyanine-sensitized titanium dioxide films, J. Photochem. Photobiol. A Chem. 156 (2003) 235–241. doi:https://doi.org/10.1016/S1010-6030(03)00008-X.

[57] G. Schlichthörl, N.G. Park, A.J. Frank, Evaluation of the Charge-Collection Efficiency of Dye-Sensitized Nanocrystalline TiO_2 Solar Cells, J. Phys. Chem. B. 103 (1999) 782–791. doi:10.1021/jp9831177.

[58] N.-G. Park, J. van de Lagemaat, A.J. Frank, Comparison of Dye-Sensitized Rutile- and Anatase-Based TiO2 Solar Cells, J. Phys. Chem. B. 104 (2000) 8989–8994. doi:10.1021/jp994365l.

[59] K. Shankar, G.K. Mor, H.E. Prakasam, S. Yoriya, M. Paulose, O.K. Varghese, C.A. Grimes, Highly-ordered TiO_2 arrays up to 220 μm in length: use in water photoelectrolysis and dye-sensitized solar cells, Nanotechnology. 18 (2007) 65707. doi:10.1088/0957-4484/18/6/065707.

[60] M. Ni, M.K.H. Leung, D.Y.C. Leung, K. Sumathy, A review and recent developments in photocatalytic water-splitting using TiO_2 for hydrogen production, Renew. Sustain. Energy Rev. 11 (2007) 401–425. doi:https://doi.org/10.1016/j.rser.2005.01.009.

[61] R. Vogel, P. Hoyer, H. Weller, Quantum-Sized PbS, CdS, Ag_2S, Sb_2S_3, and Bi_2S_3 Particles as Sensitizers for Various Nanoporous Wide-Bandgap Semiconductors, J. Phys. Chem. 98 (1994) 3183–3188. doi:10.1021/j100063a022.

[62] K.Y. Song, M.K. Park, Y.T. Kwon, H.W. Lee, W.J. Chung, W.I. Lee, Preparation of Transparent Particulate MoO_3/TiO_2 and WO_3/TiO_2 Films and Their Photocatalytic Properties, Chem. Mater. 13 (2001) 2349–2355. doi:10.1021/cm000858n.

[63] C. Wang, C. Shao, X. Zhang, Y. Liu, SnO_2 Nanostructures-TiO_2 Nanofibers Heterostructures: Controlled Fabrication and High Photocatalytic Properties, Inorg. Chem. 48 (2009) 7261–7268. doi:10.1021/ic9005983.

[64] K. Vinodgopal, I. Bedja, P. V Kamat, Nanostructured Semiconductor Films for Photocatalysis. Photoelectrochemical Behavior of SnO_2/TiO_2 Composite Systems and Its Role in Photocatalytic Degradation of a Textile Azo Dye, Chem. Mater. 8 (1996) 2180–2187. doi:10.1021/cm950425y.

[65] H. Zhang, R. Zong, J. Zhao, Y. Zhu, Dramatic Visible Photocatalytic Degradation Performances Due to Synergetic Effect of TiO_2 with PANI, Environ. Sci. Technol. 42 (2008) 3803–3807. doi:10.1021/es703037x.

[66] L. Song, R. Qiu, Y. Mo, D. Zhang, H. Wei, Y. Xiong, Photodegradation of phenol in a polymer-modified TiO_2 semiconductor particulate system under the irradiation of visible light, Catal. Commun. 8 (2007) 429–433. doi:10.1016/j.catcom.2006.07.001.

[67] H. chao Liang, X. zhong Li, Visible-induced photocatalytic reactivity of polymer-sensitized titania nanotube films, Appl. Catal. B Environ. 86 (2009) 8–17. doi:10.1016/j.apcatb.2008.07.015.

[68] S.X. Min, F. Wang, L. Feng, Y.C. Tong, Z.R. Yang, Synthesis and photocatalytic activity of TiO_2/conjugated polymer complex nanoparticles, Chinese Chem. Lett. 19 (2008) 742–746. doi:https://doi.org/10.1016/j.cclet.2008.03.016.

[69] Y. Wang, M. Zhong, F. Chen, J. Yang, Visible light photocatalytic activity of TiO_2/D-PVA for MO degradation, Appl. Catal. B Environ. 90 (2009) 249–254. doi:https://doi.org/10.1016/j.apcatb.2009.03.032.

[70] G. Li, F. Wang, P. Liu, Z. Chen, P. Lei, Z. Xu, Z. Li, Y. Ding, S. Zhang, M. Yang, Polymer dots grafted TiO2nanohybrids as high performance visible light photocatalysts, Chemosphere. 197 (2018) 526–534. doi:10.1016/j.chemosphere.2018.01.071.

[71] A. Fujishima, X. Zhang, D.A. Tryk, TiO_2 photocatalysis and related surface phenomena, Surf. Sci. Rep. 63 (2008) 515–582. doi:10.1016/j.surfrep.2008.10.001.

[72] P. Lei, F. Wang, S. Zhang, Y. Ding, J. Zhao, M. Yang, Conjugation-grafted-TiO_2 nanohybrid for high photocatalytic efficiency under visible light, ACS Appl. Mater. Interfaces. 6 (2014) 2370–2376. doi:10.1021/am4046537.

[73] A. Fujishima, K. Honda, Electronchemical photolysis at a semiconductor electrode, Nature. 238 (1972) 238. doi:https://doi.org/10.1038/238037a0.

[74] E. Filippo, C. Carlucci, A.L. Capodilupo, P. Perulli, F. Conciauro, G.A. Corrente, G. Gigli, G. Ciccarella, Facile preparation of TiO_2-polyvinyl alcohol hybrid nanoparticles with improved visible light photocatalytic activity, Appl. Surf. Sci. 331 (2015) 292–298. doi:10.1016/j.apsusc.2014.12.112.

[75] X. Hao, Z. Jin, J. Xu, S. Min, G. Lu, Functionalization of TiO_2 with graphene quantum dots for efficient photocatalytic hydrogen evolution, Superlattices Microstruct. 94 (2016) 237–244. doi:10.1016/j.spmi.2016.04.024.

[76] J. Zhang, X. Zhang, S.S. Dong, X. Zhou, S.S. Dong, N-doped carbon quantum dots/TiO_2 hybrid composites with enhanced visible light driven photocatalytic activity toward dye wastewater degradation and mechanism insight, J. Photochem. Photobiol. A Chem. 325 (2016) 104–110. doi:10.1016/j.jphotochem.2016.04.012.

[77] J. Zhang, M. Vasei, Y. Sang, H. Liu, J.P. Claverie, TiO_2@Carbon Photocatalysts: The Effect of Carbon Thickness on Catalysis, ACS Appl. Mater. Interfaces. 8 (2016) 1903–1912. doi:10.1021/acsami.5b10025.

[78] W.-C. Oh, A.-R. Jung, W.-B. Ko, O. WC, J. AR, K. WB, W.-C. Oh, A.-R. Jung, W.-B. Ko, Preparation of fullerene/TiO_2 composite and its photocatalytic effect, J. Ind. Eng. Chem. 13 (2007) 1208–1214. https://www.cheric.org/research/tech/periodicals/view.php?seq=692526.

[79] J. Wang, M. Wang, J. Xiong, C. Lu, Enhanced photocatalytic activity of a TiO_2/graphene composite by improving the reduction degree of graphene, New Carbon Mater. 30 (2015) 357–363. doi:https://doi.org/10.1016/S1872-5805(15)60195-0.

[80] J. Moon, C.Y. Yun, K.-W. Chung, M.-S. Kang, J. Yi, Photocatalytic activation of TiO_2 under visible light using Acid Red 44, Catal. Today. 87 (2003) 77–86. doi:https://doi.org/10.1016/j.cattod.2003.10.009.

[81] U. Caudillo-Flores, J. Lara-Romero, J. Zárate-Medina, M.J. Muñoz-Batista, R. Huirache-Acuña, E.M. Rivera-Muñoz, J.A. Cortés, Enhanced photocatalytic activity of MWCNT/TiO_2 heterojunction photocatalysts obtained by microwave assisted synthesis, Catal. Today. 266 (2016) 102–109. doi:10.1016/j.cattod.2015.12.005.

[82] X.F. Wang, O. Kitao, E. Hosono, H. Zhou, S. ichi Sasaki, H. Tamiaki, TiO_2- and ZnO-based solar cells using a chlorophyll a derivative sensitizer for light-harvesting and energy conversion, J. Photochem. Photobiol. A Chem. 210 (2010) 145–152. doi:10.1016/j.jphotochem.2010.01.004.

[83] G. Benk, B. Skrman, R. Wallenberg, A. Hagfeldt, V. Sundstrm, A.P. Yartsev, Particle Size and Crystallinity Dependent Electron Injection in Fluorescein 27-Sensitized TiO_2 Films, J. Phys. Chem. B. 107 (2003) 1370–1375. doi:10.1021/jp026442.

[84] D. Wang, Y. Wang, X. Li, Q. Luo, J. An, J. Yue, Sunlight photocatalytic activity of polypyrrole-TiO_2 nanocomposites prepared by “in situ” method, Catal. Commun. 9 (2008) 1162–1166. doi:10.1016/j.catcom.2007.10.027.

[85] Y. Guo, M. Zhang, Z. Zhang, Q. Li, J. Yang, Facile synthesis of a conjugation-grafted-TiO_2 nanohybrid with enhanced visible-light photocatalytic properties from nanotube titanic acid precursors, J. Nanoparticle Res. 18 (2016) 228. doi:10.1007/s11051-016-3543-6.

[86] H. Yang, J. Zhang, Y. Song, S. Xu, L. Jiang, Y. Dan, Visible light photo-catalytic activity of C-PVA/TiO_2 composites for degrading rhodamine B, Appl. Surf. Sci. 324 (2015) 645–651. doi:10.1016/j.apsusc.2014.11.002.

[87] H. Yu, Y. Zhao, C. Zhou, L. Shang, Y. Peng, Y. Cao, L.-Z. Wu, C.-H. Tung, T. Zhang, Carbon quantum dots/TiO_2 composites for efficient photocatalytic hydrogen evolution, J. Mater. Chem. A. 2 (2014) 3344. doi:10.1039/c3ta14108j.

[88] Y. Zhu, Y. Dan, Photocatalytic activity of poly(3-hexylthiophene)/titanium dioxide composites for degrading methyl orange, Sol. Energy Mater. Sol. Cells. 94 (2010) 1658–1664. doi:10.1016/j.solmat.2010.05.025.

[89] S. Min, J. Hou, Y. Lei, X. Ma, G. Lu, Facile one-step hydrothermal synthesis toward strongly coupled TiO_2/graphene quantum dots photocatalysts for efficient hydrogen evolution, Appl. Surf. Sci. 396 (2017) 1375–1382.

doi:10.1016/j.apsusc.2016.11.169.
[90] J. Li, Y. Liu, Z. Zhu, G. Zhang, T. Zou, Z. Zou, S. Zhang, D. Zeng, C. Xie, A full-sunlight-driven photocatalyst with super long-persistent energy storage ability, Sci. Rep. 3 (2013) 2409. doi:10.1038/srep02409.
[91] Y. Li, B.P. Zhang, J.X. Zhao, Z.H. Ge, X.K. Zhao, L. Zou, ZnO/carbon quantum dots heterostructure with enhanced photocatalytic properties, Appl. Surf. Sci. 279 (2013) 367–373. doi:10.1016/j.apsusc.2013.04.114.
[92] A. Qu, H. Xie, X. Xu, Y. Zhang, S. Wen, Y. Cui, High quantum yield graphene quantum dots decorated TiO_2 nanotubes for enhancing photocatalytic activity, Appl. Surf. Sci. 375 (2016) 230–241. doi:10.1016/j.apsusc.2016.03.077.
[93] M. Faisal, S. Bahadar, M.M. Rahman, A. Jamal, M.M. Abdullah, Applied Surface Science Fabrication of ZnO nanoparticles based sensitive methanol sensor and efficient photocatalyst, Appl. Surf. Sci. 258 (2012) 7515–7522. doi:10.1016/j.apsusc.2012.04.075.
[94] M. Shahid, I. Shakir, S.J. Yang, D.J. Kang, Facile synthesis of core-shell SnO_2/V_2O_5 nanowires and their efficient photocatalytic property, Mater. Chem. Phys. 124 (2010) 619–622. doi:10.1016/j.matchemphys.2010.07.023.
[95] K. Sayama, H. Hayashi, T. Arai, M. Yanagida, T. Gunji, H. Sugihara, Highly active WO_3 semiconductor photocatalyst prepared from amorphous peroxo-tungstic acid for the degradation of various organic compounds, Appl. Catal. B Environ. 94 (2010) 150–157. doi:10.1016/j.apcatb.2009.11.003.
[96] A.A. Vega, G.E. Imoberdorf, M. Mohseni, Photocatalytic degradation of 2,4-dichlorophenoxyacetic acid in a fluidized bed photoreactor with composite template-free TiO_2 photocatalyst, Appl. Catal. A Gen. 405 (2011) 120–128. doi:10.1016/j.apcata.2011.07.033.
[97] W. Chen, D. Li, L. Tian, W. Xiang, T. Wang, W. Hu, Y. Hu, S. Chen, J. Chen, Z. Dai, Synthesis of graphene quantum dots from natural polymer starch for cell imaging, Green Chem. (2018). doi:10.1039/C8GC02106F.
[98] S. Zhu, J. Zhang, L. Wang, Y. Song, G. Zhang, H. Wang, B. Yang, A general route to make non-conjugated linear polymers luminescent, Chem. Commun. 48 (2012) 10889–10891. doi:10.1039/C2CC36080B.
[99] J. Shen, Y. Zhu, X. Yang, C. Li, Magnetic composite microspheres with exposed {001} faceted TiO_2 shells: a highly active and selective visible-light photocatalyst, J. Mater. Chem. 22 (2012) 13341–13347. doi:10.1039/C2JM31998E.
[100] Z. Ding, X. Hu, G.Q. Lu, P.-L. Yue, P.F. Greenfield, Novel silica gel supported TiO_2 photocatalyst synthesized by CVD method, Langmuir. 16 (2000) 6216–6222. doi:https://doi.org/10.1021/la000119l.
[101] S. Fukahori, H. Ichiura, T. Kitaoka, H. Tanaka, Photocatalytic decomposition of bisphenol A in water using composite TiO_2-zeolite sheets prepared by a papermaking technique, Environ. Sci. Technol. 37 (2003) 1048–1051. doi:https://doi.org/10.1021/es0260115.
[102] C. Ooka, S. Akita, Y. Ohashi, T. Horiuchi, K. Suzuki, S. Komai, H. Yoshida, T. Hattori, Crystallization of hydrothermally treated TiO_2 pillars in pillared

montmorillonite for improvement of the photocatalytic activity, J. Mater. Chem. 9 (1999) 2943–2952. doi:10.1039/A901421G.

[103] X. Liu, Q. Chen, L. Lv, X. Feng, X. Meng, Preparation of transparent PVA/TiO_2 nanocomposite films with enhanced visible-light photocatalytic activity, Catal. Commun. 58 (2015) 30–33.

[104] Y. Song, J. Zhang, H. Yang, S. Xu, L. Jiang, Y. Dan, Preparation and visible light-induced photo-catalytic activity of H-PVA/TiO_2 composite loaded on glass via sol–gel method, Appl. Surf. Sci. 292 (2014) 978–985. doi:https://doi.org/10.1016/j.apsusc.2013.12.090.

[105] P. Lei, F. Wang, X. Gao, Y. Ding, S. Zhang, J. Zhao, S. Liu, M. Yang, Immobilization of TiO_2 nanoparticles in polymeric substrates by chemical bonding for multi-cycle photodegradation of organic pollutants, J. Hazard. Mater. 227–228 (2012) 185–194. doi:10.1016/j.jhazmat.2012.05.029.

[106] M. Tatzber, M. Stemmer, H. Spiegel, C. Katzlberger, G. Haberhauer, M.H. Gerzabek, An alternative method to measure carbonate in soils by FT-IR spectroscopy, Environ. Chem. Lett. 5 (2007) 9–12. doi:https://doi.org/10.1007/s10311-006-0079-5.

Acknowledgement

The work above is completely authored by Songtao Li. I would like to express my gradtitude for my mentor, Dr. Qiang Chen for his patience, motivation, enthusiasm, and immense knowledge. His guidance helped me support throughout the research and writing process.

Part 2 of this thesis was conducted at Beijing National Laboratory for Molecular Science, CAS Key Laboratory of Engineering Plastics, Institute of Chemistry, Chinese Academy of Sciences under the co-mentorship of Dr. Gen Li, a Ph. D. candidate under Dr. Feng Wang and Prof. Mingshu Yang. The idea was composed by the author. The synthesis, characterization, and data analysis in Part 2 is conducted by the author under the supervision of Dr. Gen Li acoording to ICCAS regulations on laboratory safety and instrument use. Part 2, Facile green synthesis of Degraded-PVA coated TiO_2 nanoparticles with enhanced photocatalytic activity under visible light was published in Journal of Physics and Chemistry of Solids (https://doi.org/10.1016/j.jpcs.2019.01.002). The work is written by the author and edited by Dr. Gen Li and Dr. Qiang Chen. This work was supported by the National Natural Science Foundation of China [Grant No. 51650110503, 51534007 and 51403217], the Youth Innovation Promotion Association of CAS [Grant No.2017041] and the "Strategic Priority Research Program" of the Chinese Academy of Sciences [Grant No. XDA09030200]. This work is also presented at 2019 ACS Mid-Atlantic Regional Meeting, Nano and Environmental Chemistry session.

Part 3 of this thesis was conducted at Princeton International School of Mathematics and Science mentored by Dr. Qiang Chen as a continuation of an idea initially co-developed by the author and Dr. Gen Li. The synthesis and data analysis was conducted by the author at Princeton International School of Mathematics and Science. The characterization except from SEM and TGA was conducted Princeton International School of Mathematics and Science. The SEM was conducted at Institute of Chemistry, Chinese Academy of Sciences by Dr. Gen Li and the author. The TGA was conducted at Imaging and Analysis Center, Princeton University. This part was submitted for 2019 Mercer Science and Engineering Fair and received first place of Chemistry and Materials Category.

The author is more than grateful for Dr. Gen Li for enlighting my first glance on research and his immense patience in guiding me through my first publication. The author would also like to thank Dr. Feng Wang and Prof. Mingshu Yang for granting me this opportunity of working as a summer intern in Beijing National Laboratory for Molecular Science, CAS Key Laboratory of Engineering Plastics, ICCAS.

Last but not least, the author would like to thank his parents, Prof. Xiaoxia Huang and Dr. Hongga Li, Institute of Remote Sensing and Digital Earth, CAS, for their support and encouragement through my first attempt at research.

Songtao Li

Email: barton.li@prismsus.org

Brief Introduction

I am Songtao Li, a high school senior at Princeton International School of Mathematics and Science. My major academic interests are chemistry and earth science.

Education

2008.9~2013.6	Primary School, Beijing Chaoyang Foreign Language School, Beijing, China
2013.9~2016.6	Middle school/Early Development Program, High School Affiliated to Remin University, Beijing, China
2016.6~Present	High School, Princeton International School of Mathematics and Science, NJ, U.S.

Research & Competition Experience

2016	Chinese High School Chemistry Olympiad, Beijing Area Qualifying Round, First Prize
2018.7	US Earth Science Olympiad, Senior Program, University of Vermont
2018.8	Summer Internship, Beijing National Laboratory for Molecular Science, CAS Key Laboratory of Engineering Plastics, Institute of Chemistry, Chinese Academy of Sciences, Beijing, 100190, China
2018.9~Present	Personal Research Project, Princeton International School of Mathematics and Science
2019.7~2019.8	Garcia Summer Research Program, Stony Brook University, State University of New York
2019.8	Summer Internship, Institute of Arid Ecology and Environment, School of Resources and Environmental Science, University of Xinjiang, Urumuqi, Xinjiang, 830046, China

Publications & Presentations

Li, S., Li, G., Chen, Q. & Wang, F. Facile green synthesis of Degraded-PVA coated TiO_2 nanoparticles with enhanced photocatalytic activity under visible light. *J. Phys. Chem. Solids* **129**, 92–98 (2019).

Li, S., Li, G., Chen, Q. & Wang, F. Facile green synthesis of Degraded-PVA coated TiO_2 nanoparticles with enhanced photocatalytic activity under visible light. *2019 ACS Mid-Atlantic Regional Meeting, Nano and Environmental Chemistry,* Baltimore MA, June 2019.

Sharma, P., **Li, S.,** Cai, G., Wu, S., Sharma, S.K., Rafailovich M. High Performance Citric Acid Cross-Linked Cellulose Nanofiber-Based Proton Exchange Membrane. In preparation.

Qiang 'Steven' Chen, Ph. D
Email: steven.chen@prismsus.org

Brief Introduction

I am Qiang (Steven) Chen, who graduated from Peking University with a PhD in chemistry. Now I work at the Princeton International School of Mathematics and Science (PRISMS) as a science teacher, chemistry team coach, and research mentor.

PRISMS is a private STEM-focused international high school in Princeton, New Jersey. As the founding faculty, I played a key role in designing the science curriculum in PRISMS and worked closely with the students in my chemistry team and research group, stimulated and guided them achieve excellence in Chemistry research and Chemistry Olympiad in the past few years.

I teach college-level of Inorganic Chemistry, Analytical Chemistry and Organic Chemistry in PRISMS as well. With years of educational practice in nurturing talented students in both China (HS Affiliated to Renmin University of China (人大附中, ranked as the top high school in China) and US, I accumulated ample experience in US-China science education comparison/integration, and inquiry-based curriculum designing/development.

As a research mentor, I focus on utilizing chemistry and nanotechnology in solving environmental issues. Students in my group get the opportunity to work on authentic hands-on projects, varying from formaldehyde sensing, heavy metals removal, pesticides detection, to synthesis, characterization, and functionalization of nanomaterials. They presented their research progress in academic conferences, such as the ACS Middle Atlantic Regional Meeting, the IEEE Secondary Education Conference, etc., and also got dozens of top awards in the Mercer Science and Engineering Fair.

Education

2002.9~2006.7	**B. S.** in Chemistry, Peking University, China
2006.9~2011.7	**Ph.D.** in Analytical Chemistry, Peking University, China

Working experience

2011.8-2015.7	Chemistry teacher and Chemistry team coach at RDFZ, played a key role in the designing the curriculum for the new gifted program
2015.10-now	Science teacher, Chemistry team coach, and research mentor at PRISMS

Professional Achievements

2011-2015	Guided dozens of students win top awards (gold/silver medalists) in the Chinese Chemistry Olympiad National Exam and 5 of them advance into the study camp (top50) in China

2011-2015 Won Outstanding Mentors for Chemistry Olympiad Award （突出贡献/优异成绩） by Chinese Chemistry Society from 2011 to 2014.

2016-2019 Guided 4 students win Honors/High Honors Awards (top~150 and top50) in national exam of US National Chemistry Olympiad (USNCO), and Yutong Dai advance into the study camp (top20) in both 2017 and 2018 and win a gold medal at the 50th International Chemistry Olympiad in Czech and Slovakia in 2018 (ranked in the 13th place out of around 300 students all over the world).

2016-2019 Honored by American Chemical Society in recognition of guidance and encouragement given to students who have been the national finalists in the USNCO.

2018.9 Named by Yutong Dai to be the especially influential teacher in her development, honored by the Admission Office of Massachusetts Institute of Technology (MIT).

Publications

2010-2012 *Amplified QCM-D biosensor for protein based on aptamer-functionalized gold nanoparticles,* ***Q Chen****, W Tang, D Wang, X Wu, N Li, F Liu, Biosensors and Bioelectronics 26 (2), 575-579, 103,* ***2010***

Oligonucleotide-functionalized gold nanoparticles-enhanced QCM-D sensor for mercury (II) ions with high sensitivity and tunable dynamic range, ***Q Chen****, X Wu, D Wang, W Tang, N Li, F Liu, Analyst 136 (12), 2572-2577,* ***2011***

Highly selective detection of single-nucleotide polymorphisms using a quartz crystal microbalance biosensor based on the toehold-mediated strand displacement reaction, D Wang, W Tang, X Wu, X Wang, G Chen, ***Q Chen****, N Li, F Liu, Analytical Chemistry 84 (16), 7008-7014, 81,* ***2012***

2019 *Songtao Li, Gen Li,* ***Qiang Chen****, Feng Wang, Facile green synthesis of Degraded-PVA coated TiO_2 nanoparticles with enhanced photocatalytic activity under visible light,* ***2019****, 129, 92-98, Journal of Physics and Chemistry of Solids*

本参赛团队声明所提交的论文是在指导老师指导下进行的研究工作和取得的研究成果。尽本团队所知，除了文中特别加以标注和致谢中所罗列的内容以外，论文中不包含其他人已经发表或撰写过的研究成果。若有不实之处，本人愿意承担一切相关责任。

参赛队员：李松涛　　指导老师：

2019 年 8 月 30 日